Lulu2 regulates the circumferential actomyosin tensile system in epithelial cells through p114RhoGEF

Hiroyuki Nakajima and Takuji Tanoue

Global Centers of Excellence Program for Integrative Membrane Biology, Graduate School of Medicine, Kobe University, Chuo-ku, Kobe 650-0017, Japan

Myosin II–driven mechanical forces control epithelial cell shape and morphogenesis. In particular, the circumferential actomyosin belt, which is located along apical cell–cell junctions, regulates many cellular processes. Despite its importance, the molecular mechanisms regulating the belt are not fully understood. In this paper, we characterize Lulu2, a FERM (4.1 protein, ezrin, radixin, moesin) domain–containing molecule homologous to *Drosophila melanogaster* Yurt, as an important regulator. In epithelial cells, Lulu2 is localized along apical cell–cell boundaries, and Lulu2 depletion by ribonucleic acid interference results in disorganization of the circumferential actomyosin belt. In its regulation of the belt, Lulu2 interacts with and activates p114RhoGEF, a Rho-specific guanine nucleotide exchanging factor (GEF), at apical cell–cell junctions. This interaction is negatively regulated via phosphorylation events in the FERM-adjacent domain of Lulu2 catalyzed by atypical protein kinase C. We further found that Patj, an apical cell polarity regulator, recruits p114RhoGEF to apical cell–cell boundaries via PDZ (PSD-95/Dlg/ZO-1) domain–mediated interaction. These findings therefore reveal a novel molecular system regulating the circumferential actomyosin belt in epithelial cells.

Introduction

Mechanical forces generated in epithelial cells regulate several cellular processes, including apical constriction, cell intercalation, planar cell polarity regulation, cell sorting, tension sensing, and the formation and maintenance of the adherens junction (Owaribe et al., 1981; Ivanov et al., 2004, 2007; Shewan et al., 2005; Miyake et al., 2006; Lecuit and Lenne, 2007; Yamazaki et al., 2008; Zallen and Blankenship, 2008; le Duc et al., 2010; Smutny et al., 2010; Smutny and Yap, 2010; Yonemura et al., 2010). The forces themselves are mainly generated by an F-actin–myosin II bundle called the circumferential actomyosin belt, which is positioned in the apical portion of the cells as a ringlike structure along apical cell–cell junctions (tight and adherens junctions in vertebrates; Owaribe et al., 1981; Yamazaki et al., 2008; Smutny et al., 2010; Yonemura et al., 2010). Recent studies identified some molecular pathways regulating this: for example, the Rho–Rock and Rap1 pathways were reported to be responsible for proper organization of myosin II isoforms along apical cell–cell junctions (Smutny et al., 2010). As another example, shroom3 was reported to regulate myosin II activity by recruiting Rock to apical cell–cell junctions, thereby inducing apical constriction (Nishimura and Takeichi, 2008). E-cadherin, an adherens junctional component, is required for proper organization of the circumferential actomyosin belt (Smutny et al., 2010; Yano et al., 2011). ZO-1 and ZO-2, tight junctional components, are also required (Yamazaki et al., 2008); however, the detailed molecular network regulating the circumferential actomyosin belt is not completely understood.

Our previous study demonstrated that Lulu1 and 2 (also known as Epb41l5 and Epb41l4b/Ehm2, respectively) are potent activators of cortical myosin II contractile forces in epithelial cells (Nakajima and Tanoue, 2010). They commonly have a FERM (4.1 protein, ezrin, radixin, moesin) and a FERM-adjacent (FA) domain, although other portions beyond these domains do not resemble each other (Shimizu et al., 2000; Lee et al., 2007; Hirano et al., 2008). From sequence

Correspondence to Takuji Tanoue: tanoue@med.kobe-u.ac.jp

Abbreviations used in this paper: aPKC, atypical PKC; CBB, Coomassie brilliant blue; CMV, cytomegalovirus; DN, dominant negative; FA, FERM adjacent; GEF, guanine nucleotide exchanging factor; LC, liquid chromatography; MBP, maltose-binding protein; MRLC, myosin regulatory light chain; MS, mass spectrometry; PBM, PDZ domain–binding motif; PH, pleckstrin homology.

The Rockefeller University Press $30.00
J. Cell Biol. Vol. 195 No. 2 245–261
www.jcb.org/cgi/doi/10.1083/jcb.201104118

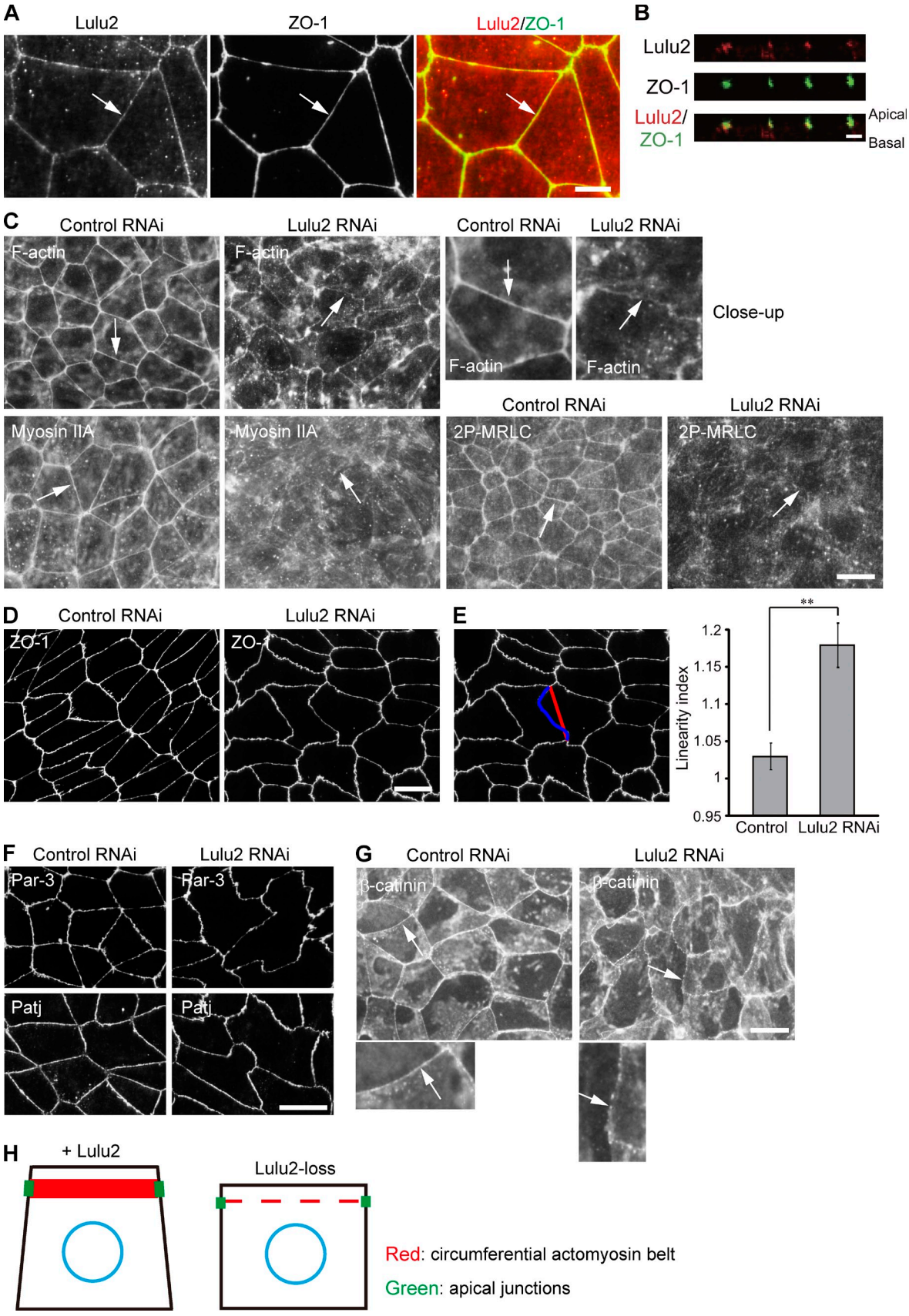

Figure 1. **Lulu2 accumulates along apical cell–cell boundaries and regulates the circumferential actomyosin belt.** (A) DLD-1 cells doubly immunostained for Lulu2 and ZO-1. Lulu2 accumulates along cell–cell boundaries overlapping ZO-1 (arrows). (B) Vertical images of DLD-1 cells doubly immunostained for Lulu2 and ZO-1. (C and D) DLD-1 cells treated with control siRNA or Lulu2 siRNA-1 were stained for F-actin, myosin IIA, diphosphorylated MRLC

similarity, Lulus are thought to be mammalian counterparts of *Drosophila melanogaster* Yurt, which was reported to be a negative regulator of apical membrane size in epithelial cells (Hoover and Bryant, 2002; Laprise et al., 2006, 2009). This Yurt activity was attributed to its negative regulation of Crumbs, which are apical membrane regulators (Laprise et al., 2006). Zebrafish Moe, the sole Lulu molecule in the species, participates in layering of the retina and inflation of the brain ventricles as well as restricting the photoreceptor apical domain (Jensen and Westerfield, 2004; Hsu et al., 2006). Moe also interacts with and negatively regulates Crumbs, thereby restricting apical membrane size in epithelial structures (Hsu et al., 2006). Mammalian Lulus, however, regulate myosin II activity rather than Crumbs activity: overexpression of Lulu1 or 2 in epithelial cells resulted in strong accumulation of F-actin and myosin II along apical cell–cell junctions, thereby inducing apical constriction in the cells (Nakajima and Tanoue, 2010). This activity of Lulu2 is much higher than that of Lulu1; therefore, Lulu2 is a good candidate molecule regulating the circumferential actomyosin belt. However, we did not explore the detailed molecular mechanisms of Lulu2 activity in the previous study, and here, we further study Lulu2 from cellular and molecular aspects.

We report that Lulu2 is a regulator of the circumferential actomyosin belt in epithelial cells. Lulu2 accumulates along apical cell–cell boundaries, overlapping ZO-1, and its depletion results in disorganization of the circumferential actomyosin belt. Lulu2 interacts with and activates the catalytic activity of p114RhoGEF, a Rho-specific guanine nucleotide exchanging factor (GEF), at apical cell–cell boundaries, thereby regulating the integrity of the circumferential actomyosin belt. In addition, Lulu2 is negatively regulated in terms of its binding ability to p114RhoGEF by phosphorylation in the FA domain, which is catalyzed by atypical PKC (aPKC). We further show that p114RhoGEF is recruited to apical cell–cell boundaries by Patj, an apicobasal cell polarity regulator. We thus propose that this Lulu2-p114RhoGEF system regulates the circumferential actomyosin belt in epithelial cells.

Results

Lulu2 accumulates along apical cell–cell boundaries overlapping ZO-1 and regulates the circumferential actomyosin belt in epithelial cells

We began by examining the localization of endogenous Lulu2 in DLD-1 cells, which exhibit the characteristic morphology of polarized epithelial cells with a well-developed circumferential actomyosin belt (Fig. S1), and found that Lulu2 accumulated along apical cell–cell boundaries, overlapping ZO-1, a tight junctional marker (Fig. 1, A and B; and Fig. S2, A–D, for the specificity of the antibody). Lulu2 was also detected in the cytoplasm as dots (Fig. 1 A), which we did not characterize further in this study. In addition, as DLD-1 cells mainly express the short form of Lulu2 (unpublished data), it was used in this study.

To understand the role of Lulu2 in the epithelial cell structure, we conducted Lulu2 RNAi experiments using DLD-1 cells (Fig. S2, C and D, RNAi). Throughout this study, we routinely confirmed the results of all the RNAi experiments by using two different siRNAs targeting each molecule, although we present the data of one siRNA for one molecule to avoid redundancy. Control RNAi cells exhibited a well-developed circumferential actomyosin belt, indicated by staining for F-actin and myosin IIA (Fig. 1 C). In Lulu2-depleted cells, in contrast, it became significantly thin with concomitant loss of phosphorylated myosin regulatory light chain (MRLC) from cell–cell boundaries (Fig. 1 C). These Lulu2-depleted cells, however, retained an apparently normal tight junction marked by ZO-1 staining, although cell–cell borders located by the staining became overly bent and less strained in Lulu2-depleted cells than controls (Fig. 1, D and E). This might have been caused by loss of apical tension generated by the circumferential actomyosin belt in Lulu2-depleted cells. In addition, other tight junctional molecules, including ZO-2, cingulin, Par3, and Patj, also apparently accumulated normally along cell–cell boundaries, further suggesting that Lulu2 might not regulate the localization of tight junctional molecules (Fig. 1 F and not depicted). In accordance with other studies that state the circumferential actomyosin belt regulates adherens junction (Ivanov et al., 2004, 2007; Shewan et al., 2005; Miyake et al., 2006; Smutny et al., 2010), in Lulu2-depleted cells, β-catenin, a component of adherens junction, became discontinuously localized at the level of zonula adherens (Fig. 1 G). These results indicate that Lulu2 accumulates along apical cell–cell boundaries and regulates the circumferential actomyosin belt (Fig. 1 H).

Lulu2 interacts with p114RhoGEF

To understand the molecular mechanism downstream of Lulu2, we screened for interacting molecules by a GST pull-down assay using a GST-fused Lulu2 FERM-FA followed by liquid chromatography (LC)-mass spectrometry (MS)/MS analyses (Fig. 2 A, FERM-FA). Adaptin δ, HSP70, ribosomal protein L4, CWC22 splicing factor, heterogeneous nuclear riboprotein U, and p114RhoGEF were identified by MS/MS (unpublished data). Among them, we focused on p114RhoGEF, as it is a Rho-specific Dbl family RhoGEF (Niu et al., 2003; Nagata and Inagaki, 2005; Tsuji et al., 2010; Terry et al., 2011), a good candidate molecule downstream of Lulu2. We first

(2P-MRLC; C), or ZO-1 (D). Arrows show cell–cell boundaries. (E) Quantification of junction linearity. Junction length (blue) and the distance between vertices (red) were measured in Lulu2-depleted cells or control cells. Linearity index is defined by the ratio of junction length to the distance between vertices. Error bars indicate SD. $n = 3$ independent experiments, in each of which >50 junctions were measured. **, $P < 0.001$ by Student's t test. (F) DLD-1 cells treated with control siRNA or Lulu2 siRNA-1 were stained for Par3 or Patj. (G) DLD-1 cells treated with control siRNA or Lulu2 siRNA-1 were immunostained for β-catenin. Arrows show zonula adherens. (bottom) Close-up views are also shown. (H) Lulu2 loss results in attenuation of the circumferential actomyosin belt. Bars: (A) 10 µm; (B) 2 µm; (C, D, F, and G) 20 µm.

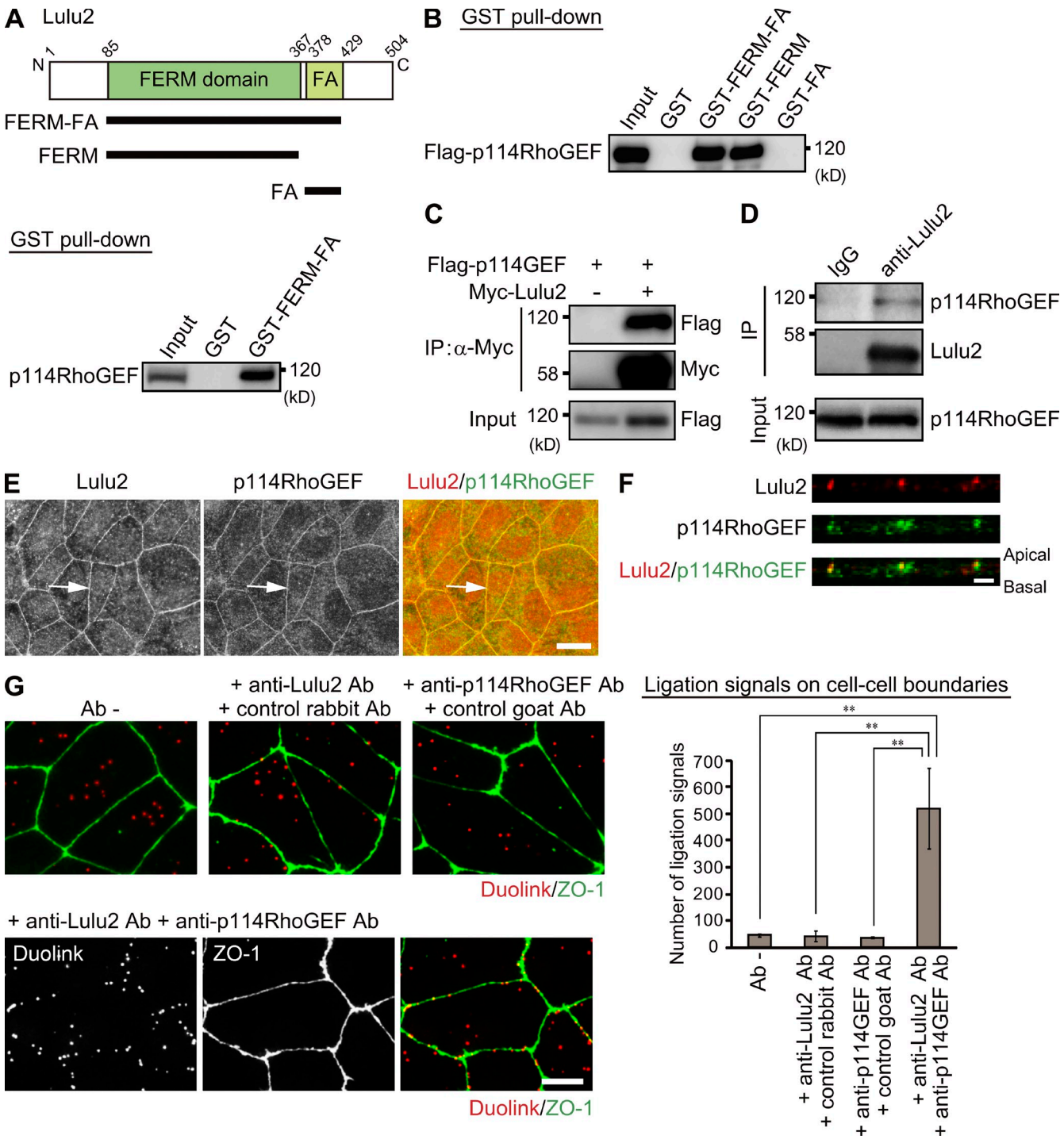

Figure 2. **Lulu2 interacts with p114RhoGEF.** (A, top schematic) Lulu2 has a FERM and a FERM adjacent (FA) domain. Amino acid numbers of mouse Lulu2 are indicated. Lysates of DLD-1 cells were examined for GST pull-down assays using GST or GST-FERM-FA. Endogenous p114RhoGEF was detected by immunoblotting. N, N terminus; C, C terminus. (B) Lysates of MDCK cells transfected with Flag-p114RhoGEF were examined for GST pull-down assays using GST, GST-FERM-FA, GST-FERM, or GST-FA (Fig. S4 B). (C) Lysates of MDCK cells cotransfected with the indicated combinations of constructs were immunoprecipitated (IP) with anti-Myc antibody. (top) Coprecipitated Flag-p114RhoGEF was detected by immunoblotting with anti-Flag antibody. Comparable amounts of Flag-p114RhoGEF were expressed (Input). (D) Lysates of DLD-1 cells were immunoprecipitated with control rabbit IgG or rabbit anti-Lulu2 antibody. Coprecipitated endogenous p114RhoGEF was detected by immunoblotting with anti-p114RhoGEF antibody. Characterization of the rabbit anti-Lulu2 antibody used is described in Fig. S2 (E and F). (E and F) DLD-1 cells doubly immunostained for Lulu2 and p114RhoGEF. Vertical images are shown in F. p114RhoGEF overlaps Lulu2 (arrows). (G) The in situ proximity ligation assay in DLD-1 cells. The assay was performed using goat anti-Lulu2 and rabbit anti-p114RhoGEF antibodies (Ab). ZO-1 was also stained using mouse anti–ZO-1 antibody to identify cell–cell boundaries. The ligation signals (red) were detected as dots at cell–cell boundaries in the samples incubated with anti-Lulu2 and anti-p114RhoGEF antibodies but scarcely detected in those incubated with anti-Lulu2 antibody and control rabbit IgG or anti-p114RhoGEF antibody and control goat IgG, suggesting that Lulu2 interacts with p114RhoGEF at cell–cell boundaries. Cytoplasmic dots are nonspecific signals in DLD-1 cells. Quantification of numbers of ligation dots at 100 cell–cell boundaries is shown in the right graph. $n = 3$ independent experiments, in each of which 100 cell–cell boundaries were examined. Error bars indicate SD. **, $P < 0.01$ by Student's t test. Bars: (E) 20 µm; (F) 2 µm; (G) 10 µm.

confirmed this MS/MS result by immunoblotting using a specific antibody for p114RhoGEF (Fig. 2 A and Fig. S3, A–D, for the specificity of the antibody). By narrowing down the region of Lulu2 for binding to p114RhoGEF, we identified the FERM domain to be necessary and sufficient for binding (Fig. 2 B and Fig. S4 B). In this study, we mainly used MDCK cells to examine interactions of exogenously expressed molecules because MDCK cells are more efficiently transfected with plasmids than DLD-1 cells, and MDCK cells are expected to have components for Lulu2 to function because Lulu2 induces strong apical constriction in MDCK cells (Nakajima and Tanoue, 2010). The interaction between Myc-tagged full-length Lulu2 and Flag-tagged full-length p114RhoGEF was also detected by a coexpression and coimmunoprecipitation assay (Fig. 2 C). Furthermore, endogenous p114RhoGEF was coimmunoprecipitated with endogenous Lulu2 in DLD-1 cells (Fig. 2 D and Fig. S2, E and F). Recently, it was reported that p114RhoGEF regulates RhoA activity at apical cell–cell junctions in epithelial cells (Terry et al., 2011). We then examined the localization of p114RhoGEF in DLD-1 cells and found it to be well colocalized with Lulu2 along apical cell–cell boundaries (Fig. 2, E and F). We further tested the interaction between endogenous Lulu2 and p114RhoGEF along cell–cell boundaries by an in situ proximity ligation assay. The ligation signals were detected at cell–cell boundaries overlapping ZO-1, suggesting that Lulu2 might interact with p114RhoGEF there (Fig. 2 G). These results combined indicate that Lulu2 might interact with p114RhoGEF along apical cell–cell boundaries in epithelial cells.

Lulu2 binds to the C-terminal portion of p114RhoGEF, probably via direct interaction

We next determined the Lulu2 binding region in p114RhoGEF. p114RhoGEF has Dbl homology and pleckstrin homology (PH) domains, which are necessary for its catalytic activity, followed by a coiled-coil region and a potential PDZ (PSD-95/Dlg/ZO-1) domain–binding motif (PBM) in its C-terminal tail (Fig. 3 A). From sequence similarity, p114RhoGEF and three other Dbl RhoGEFs, p190 RhoGEF, AKAP13/Lbc, and GEF-H1, form a subfamily (Fig. 3 D; Schmidt and Hall, 2002; García-Mata and Burridge, 2007). To narrow down the region of p114RhoGEF interacting with Lulu2, we tested various truncated mutants of p114RhoGEF for binding to Lulu2 by GST pull-down assays using GST-FERM and identified that the region C terminal to the coiled-coil region without the PBM (C4ΔPBM) was necessary and sufficient for interacting with Lulu2 (Fig. 3 A). We confirmed this result by conducting additional pull-down assays using GST-fused truncated mutants of p114RhoGEF. Myc-tagged full-length Lulu2 expressed in the cells was efficiently pulled down by GST-C2, -C4, or -C4ΔPBM but not by GST, GST-N, or -C1 of p114RhoGEF (Fig. 3 B and Fig. S4 B). Furthermore, p114RhoGEF C4ΔPBM proteins bound to Lulu2 FERM proteins in vitro (Fig. 3 C and Fig. S4, B and C). These results together indicate that Lulu2 might bind to the C4ΔPBM of p114RhoGEF.

Because the Lulu2-interacting portion is poorly conserved among the four members (Fig. 3 D), these results suggest specific interactions between Lulu2 and p114RhoGEF in the subfamily. Supporting this notion, Lulu2 scarcely bound to GEF-H1 (unpublished data).

p114RhoGEF is necessary for Lulu2 activity in the cells and regulates the circumferential actomyosin belt

To examine whether p114RhoGEF was involved in myosin II regulation by Lulu2, we used Lulu2-expressing MDCK cells, which were shown in the previous study to exhibit strong myosin II–dependent apical constriction when mixed with nonexpressing parental cells (Nakajima and Tanoue, 2010). By RNAi-mediated p114RhoGEF depletion, apical constriction of Lulu2-expressing MDCK cells became impaired, indicating that p114RhoGEF is necessary for myosin II activation by Lulu2 (Fig. 4, A and B; and Fig. S3 E, RNAi). Incomplete inhibition of apical constriction by p114RhoGEF RNAi might be because of incomplete loss of p114RhoGEF in Lulu2-expressing cells by our RNAi. A trace signal of p114RhoGEF staining was still detected after RNAi treatment in Lulu2-expressing cells (unpublished data).

To elucidate the role of p114RhoGEF in the organization of the circumferential actomyosin belt in DLD-1 cells, we examined the phenotype of p114RhoGEF-depleted DLD-1 cells (Fig. S3, C and D, RNAi). In p114RhoGEF-depleted DLD-1 cells, the circumferential actomyosin belt was severely disorganized because accumulation of F-actin, myosin IIA, and phospho-MRLC along apical cell–cell junctions was markedly reduced (Fig. 4 C). ZO-1 accumulation was not affected by p114RhoGEF depletion, although cell–cell borders became overly bent and less strained as was the case with Lulu2-depleted cells (Fig. 4, D and E). These results indicate that p114RhoGEF is a regulator of the circumferential actomyosin belt. As p114RhoGEF is a Rho-specific GEF, we postulated that it might be regulated by Lulu2.

Catalytic activity of p114RhoGEF is up-regulated by Lulu2 in vitro

The next question was therefore how Lulu2 regulates p114-RhoGEF. Because Lulu2 depletion by RNAi in DLD-1 cells did not markedly reduce the accumulation of p114-RhoGEF at cell–cell boundaries (unpublished data), Lulu2 might not target it there. We thus hypothesized that Lulu2 might enhance the catalytic activity of p114RhoGEF. To test this idea, we measured the catalytic activity of p114RhoGEF in the presence or absence of Lulu2 in vitro. As both full-length Lulu2 and p114RhoGEF proteins were hardly obtained in bacteria, we prepared full-length proteins from lysates of MDCK cells expressing Myc-Lulu2 or Flag-p114RhoGEF by immunoprecipitation with antibodies for the tags followed by elution with peptides for the tags (Fig. 4 F). We first confirmed that the prepared p114RhoGEF has GEF activity toward RhoA as previously reported (Fig. 4 F; Nagata and Inagaki, 2005). When p114RhoGEF was mixed with Lulu2 in the assay, its GEF activity was up-regulated (Fig. 4 F), suggesting that Lulu2 activates p114RhoGEF. Although further structural studies, such as determination of the three-dimensional structures of both molecules in a complex,

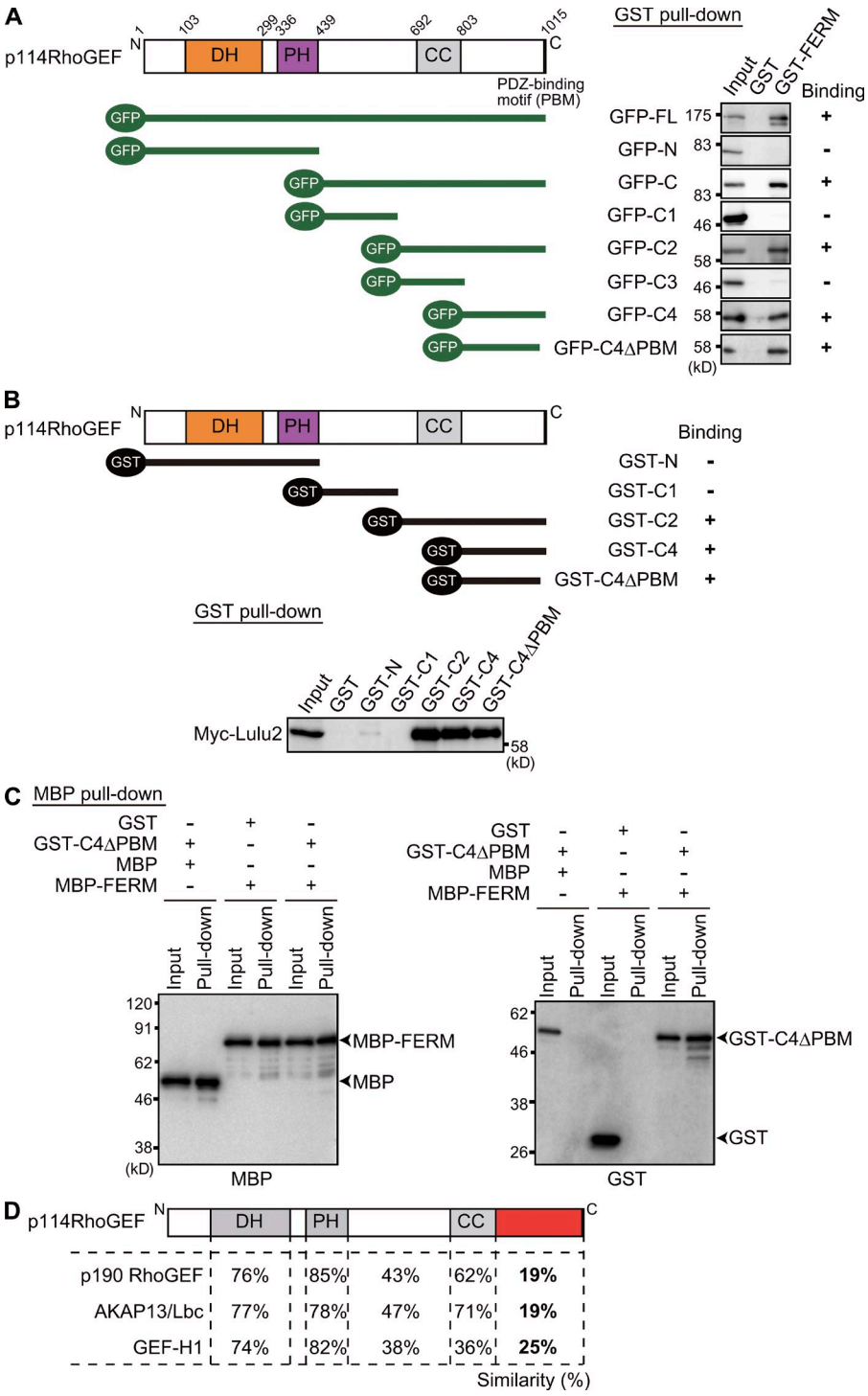

Figure 3. **Lulu2 binds to the C-terminal portion of p114RhoGEF.** (A) Amino acid numbers of human p114RhoGEF are indicated. EGFP-tagged full-length (FL) or various truncated forms of p114RhoGEF were expressed in MDCK cells and examined for binding to GST or GST-FERM by GST pull-down assays. C4ΔPBM: C4 without last six amino acid residues. See Materials and methods for the details of the truncated forms. DH, Dbl homology domain; PH, pleckstrin homology domain; CC, coiled-coil region. (B) Myc-tagged full-length Lulu2 was expressed in MDCK cells and examined for binding to GST-tagged truncated forms of p114RhoGEF by GST pull-down assays. GST fusion proteins used are shown in Fig. S4 B. (C) GST-fused C4ΔPBM or GST was mixed and incubated with MBP-fused FERM or MBP in vitro and precipitated with amylose resin (MBP pull-down). Precipitated MBP or GST proteins (pull-down) were detected using anti-MBP or -GST antibodies. Proteins used are shown in Fig. S4 B. See Materials and methods for details. (D) The Lulu2 binding region (red) in p114RhoGEF is poorly conserved among four Dbl family GEFs. Numbers indicate similarity between p114RhoGEF and the others. N, N terminus; C, C terminus.

are needed, we can speculate here that the binding of Lulu2 might cause some conformational change in p114RhoGEF to enhance its catalytic activity.

The PBM of p114RhoGEF is required for targeting of p114RhoGEF to apical cell–cell boundaries

Because Lulu2 does not recruit p114RhoGEF to apical cell–cell boundaries, we next investigated the targeting mechanism of p114RhoGEF there. We first roughly mapped the region of p114RhoGEF required for its localization at apical cell–cell boundaries in DLD-1 cells. The full-length and C-terminal portion were recruited to apical cell–cell boundaries marked by ZO-1 staining, whereas the N-terminal portion was not (Fig. 5). We thus considered that a potential PBM in its C-terminal tail might be responsible for its targeting and tested this possibility. It was found that the mutant form of p114RhoGEF that lacks the potential PBM was not recruited to apical cell–cell boundaries (Fig. 5). Therefore, p114RhoGEF might be targeted to apical cell–cell boundaries via PDZ domain–mediated interaction.

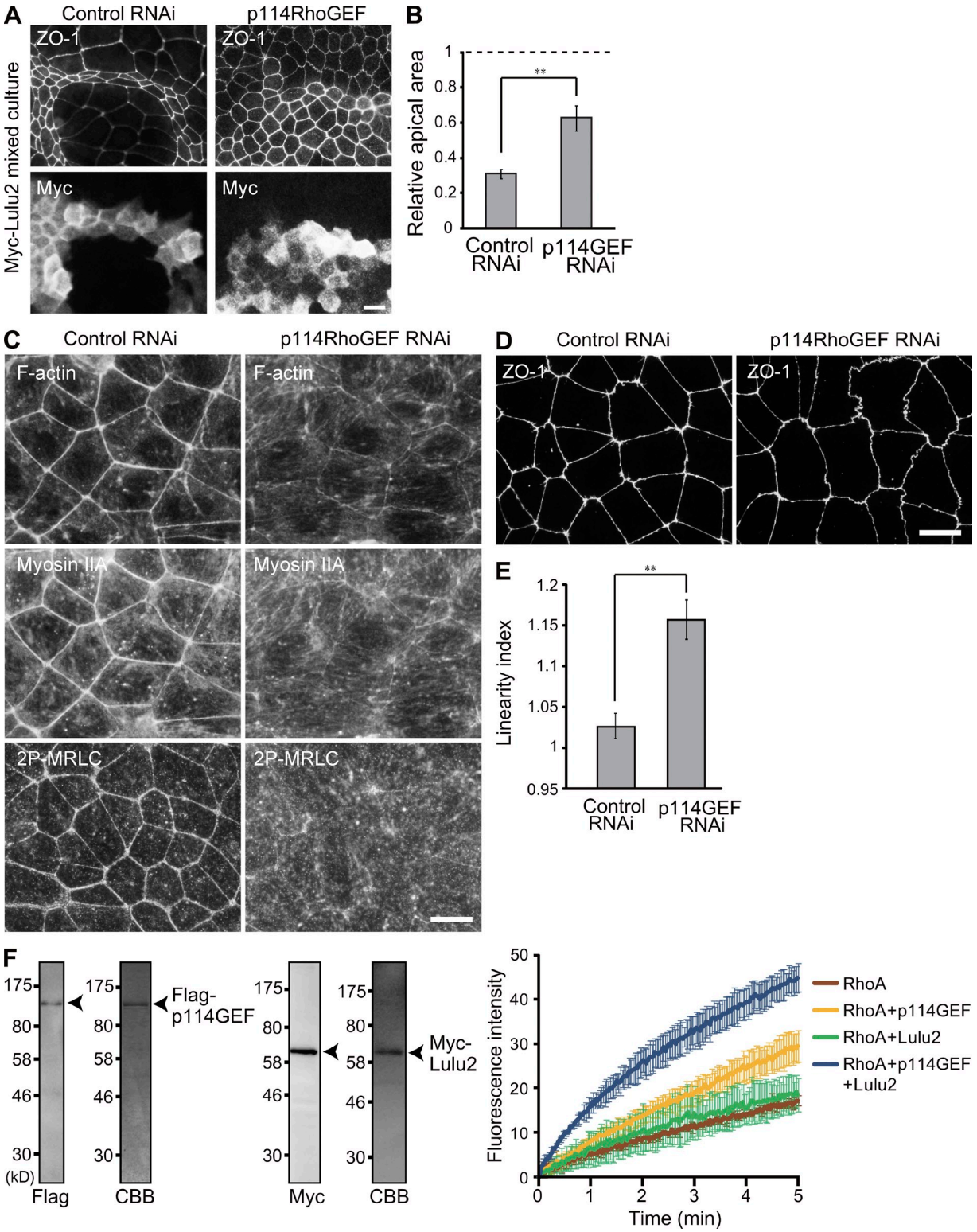

Figure 4. **p114RhoGEF is necessary for Lulu2 activity in the cells and is up-regulated by Lulu2 in vitro.** (A and B) Mixed cell cultures of parental and Myc-Lulu2–expressing MDCK cells were treated with control siRNA or p114RhoGEF siRNA-1. (A) Cells were doubly immunostained for Myc and ZO-1. Note that Lulu2-expressing cells have higher cell heights than parental cells, resulting in the out of focus images of the parental cells. (B) Quantification of relative apical areas in Lulu2-expressing cells normalized by those in neighboring cells. The dotted line marks where the relative apical area is 1. $n = 3$ independent experiments, in each of which >100 cells were measured. **, $P < 0.01$ by Student's t test. (C and D) DLD-1 cells treated with control siRNA or p114RhoGEF siRNA-1 were stained for F-actin, myosin IIA, diphosphorylated MRLC (2P-MRLC; C), or ZO-1 (D). (E) Linearity index was quantified as in Fig. 1 E. (F) In vitro guanine nucleotide exchange reaction of p114RhoGEF toward RhoA was monitored as an increase in fluorescence, which is indicative of the binding of *N*-methylanthraniloyl–GTP to small GTPases. p114RhoGEF possesses GEF activity toward RhoA (yellow), which is up-regulated in the presence of Lulu2 (blue). Three independent experiments were quantified. (left) The proteins used are detected by Western blotting (WB) with anti-Flag or anti-Myc antibody or stained with CBB. See Materials and methods for details. Error bars indicate SD. Bars, 20 µm.

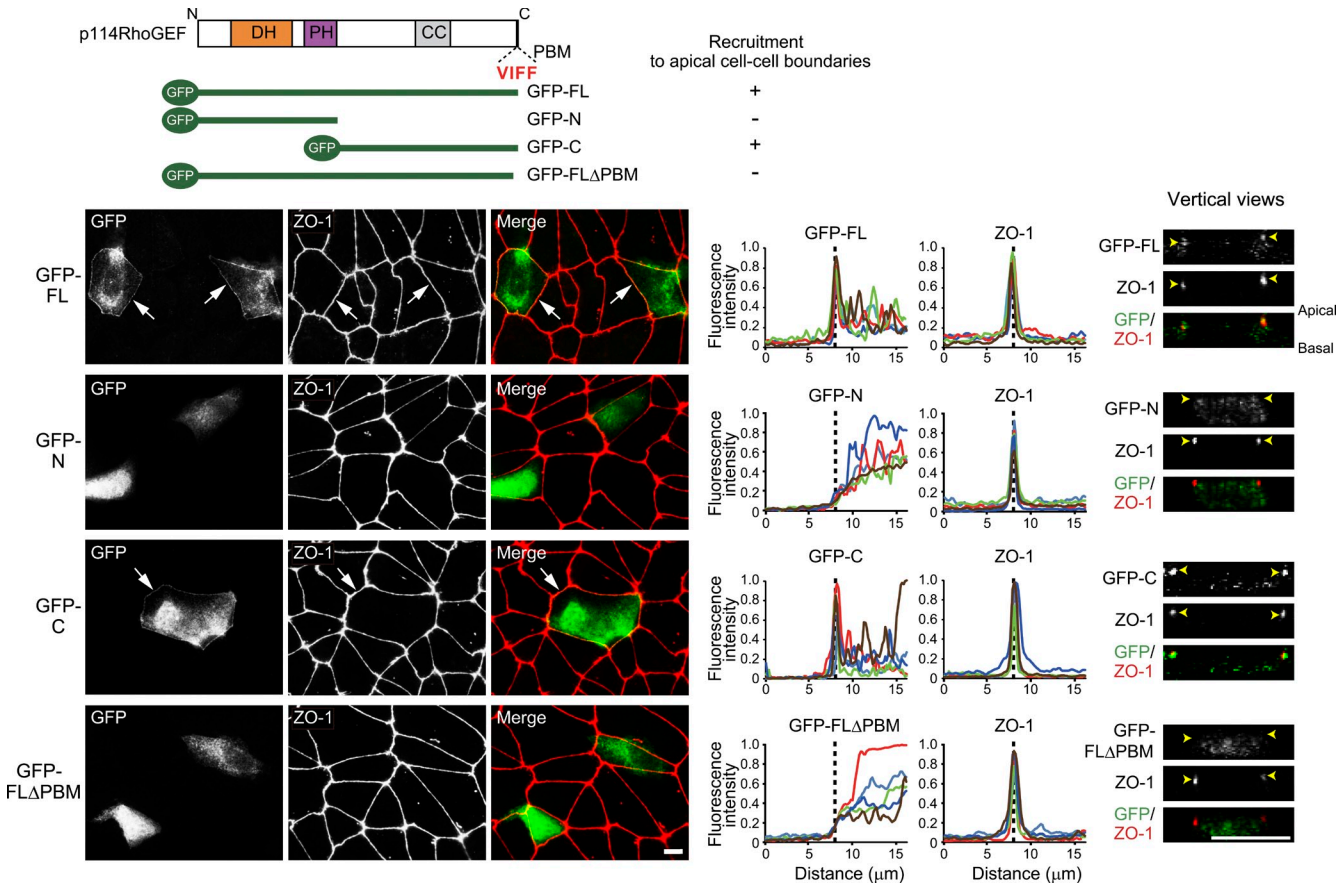

Figure 5. **The C-terminal PBM is necessary for p114RhoGEF to be localized at apical cell–cell boundaries.** (top schematic) p114RhoGEF possesses a potential PBM (VIFF) in its C-terminal tail. DLD-1 cells transfected with EGFP-tagged full-length p114RhoGEF (FL), N-terminal portion of p114RhoGEF (N), C-terminal portion of p114RhoGEF (C), or p114RhoGEFΔPBM (FLΔPBM), in which its last six amino acid residues were deleted, were doubly immunostained for EGFP and ZO-1. Fluorescence intensity of the EGFP or ZO-1 signal was scanned across cell–cell boundaries between control and EGFP-expressing cells (left and right of dotted lines, respectively). Five different cell–cell boundaries were measured (shown in different colors). (right) Vertical images are also shown. Although full-length and C-terminal p114RhoGEF accumulate along apical cell–cell boundaries, overlapping ZO-1, N-terminal p114RhoGEF, and FLΔPBM do not. Arrows and arrowheads show cell–cell boundaries marked by ZO-1. Bars, 10 μm.

Patj recruits p114RhoGEF to apical cell–cell boundaries

To identify the molecule targeting p114RhoGEF, we tested several PDZ domain–containing molecules known to be localized at cell–cell boundaries for binding to p114RhoGEF by GST pull-down assays using the C2 fragment of p114RhoGEF. Among them, it was found that Patj and Par3, well-known apical cell polarity regulators (Suzuki and Ohno, 2006; Goldstein and Macara, 2007; Assémat et al., 2008; Martin-Belmonte and Mostov, 2008; Pieczynski and Margolis, 2011), bound to the C2 fragment (Fig. S4 A). The former has 10 PDZ domains, and the latter has three PDZ domains. Both Myc-tagged Patj and Par3 expressed in the cells efficiently bound to the C2 fragment of p114RhoGEF, and these interactions depended on the putative PBM of p114RhoGEF (Fig. 6 A and Fig. S4 B). To know which molecule actually targets p114RhoGEF in the cells, we examined the relationship among p114RhoGEF, Patj, and Par3 in terms of their localization. As previously reported in other cell types (Suzuki et al., 2001; Lemmers et al., 2002; Shin et al., 2005; Adachi et al., 2009), in DLD-1 cells, both Patj and Par3 overlap ZO-1 (unpublished data). In Patj-depleted cells, continuous ZO-1 staining was not affected, whereas it became partially fragmented in Par3-depleted cells (Fig. 6 B and Fig. S3, F, G, I, and J, RNAi). In both Par3- and Patj-depleted cells, p114RhoGEF mostly disappeared from cell–cell boundaries marked by ZO-1 staining (Fig. 6 B). In Patj-depleted cells, Par3 localization was not altered: Par3 still overlaps ZO-1 (Fig. 6 C). However, in Par3-depleted cells, Patj disappeared from cell–cell boundaries where ZO-1 accumulated (Fig. 6 D). These results suggest that Par3 is upstream of Patj, and Patj is upstream of p114RhoGEF in terms of accumulation at cell–cell boundaries. In addition, the total expression level of p114RhoGEF protein was not affected by Patj depletion (Fig. 6 E), indicating that the delocalization of p114RhoGEF in Patj-depleted cells is not caused by down-regulation of the total protein level of p114RhoGEF. The interaction between GFP-tagged full-length p114RhoGEF and Myc-tagged full-length Patj was detected in a coimmunoprecipitation assay (Fig. 6 F). This interaction, as expected, required the C-terminal PBM of p114RhoGEF (Fig. 6 F). Furthermore, endogenous p114RhoGEF was coimmunoprecipitated with endogenous Patj (Fig. 6 G). In addition, cingulin, which was recently reported to bind to the PH domain of p114RhoGEF and to be necessary for p114RhoGEF localization along cell–cell boundaries (Terry et al., 2011), remained

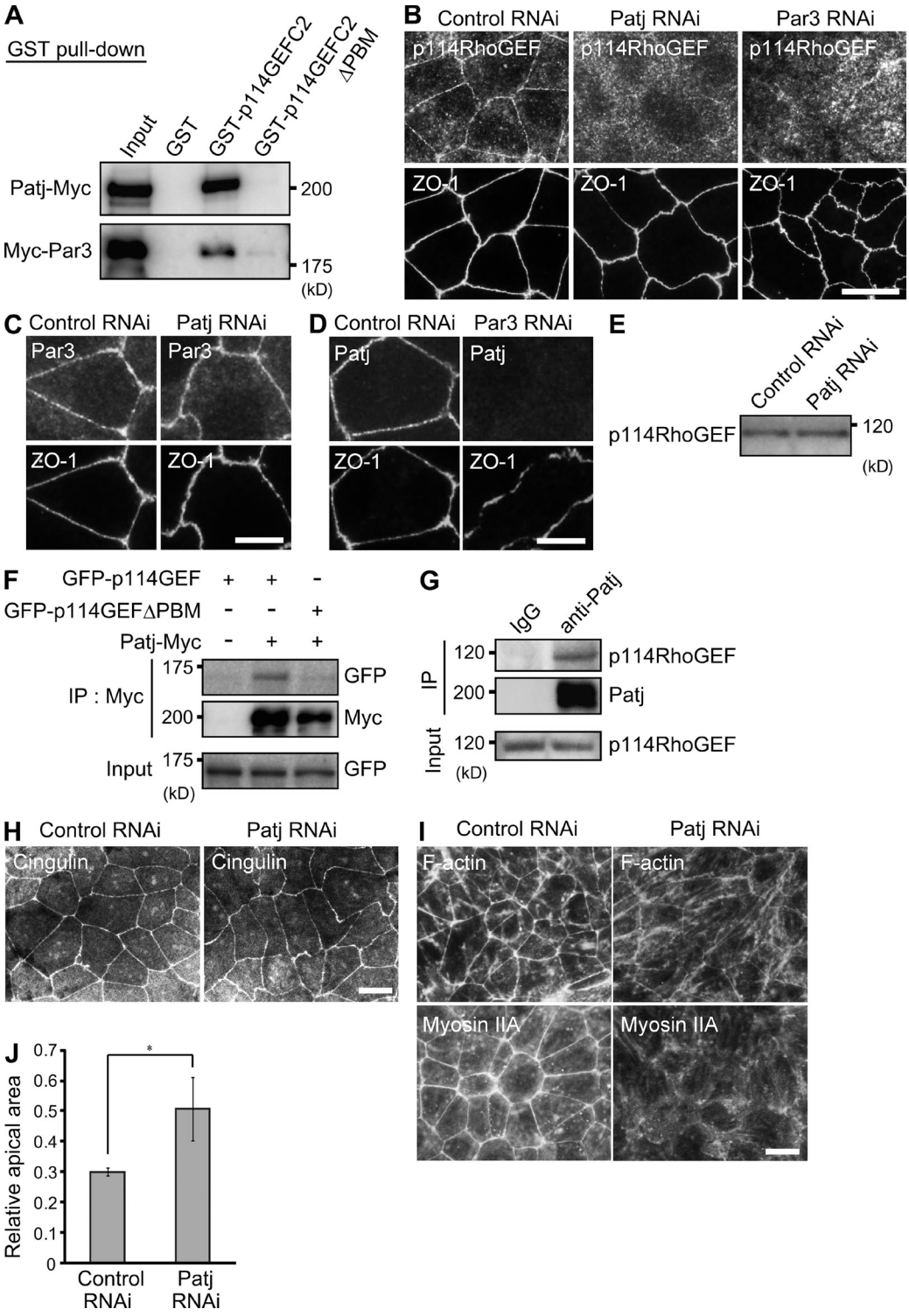

Figure 6. **Patj is necessary for p114RhoGEF to be recruited to apical cell–cell boundaries and regulates the circumferential actomyosin belt.** (A) GST pull-down was performed with GST, GST-p114RhoGEF C2, or GST-p114RhoGEF C2ΔPBM (Fig. 3 A, C2). Myc-tagged Patj and Par3 expressed in MDCK cells were examined. (B) DLD-1 cells treated with control siRNA, Patj, or Par3 siRNA-1 were doubly immunostained for p114RhoGEF and ZO-1. (C) DLD-1 cells treated with control siRNA or Patj siRNA-1 were doubly immunostained for Par3 and ZO-1. (D) DLD-1 cells treated with control siRNA or Par3 siRNA-1 were doubly immunostained for Patj and ZO-1. (E) DLD-1 cells treated with control siRNA or Patj siRNA-1 were analyzed by immunoblotting with anti-p114RhoGEF antibody. (F) Lysates of MDCK cells cotransfected with the indicated combinations of constructs were immunoprecipitated (IP) with anti-Myc antibody. (top, GFP) Coimmunoprecipitated EGFP-p114RhoGEF was detected. Comparable amounts of EGFP-p114RhoGEF or EGFP-p114RhoGEFΔPBM were expressed (Input). (G) Lysates of DLD-1 cells were immunoprecipitated with anti-Patj antibody. Endogenous p114RhoGEF was detected. (H and I) DLD-1 cells treated with control siRNA or Patj siRNA-1 were stained for cingulin (H), F-actin, or myosin IIA (I). (J) Mixed cell cultures of parental and Myc-Lulu2–expressing MDCK cells were treated with control siRNA or Patj siRNA-1. Relative apical areas in Lulu2-expressing cells normalized by those in neighboring cells were quantified as in Fig. 4 B. $n = 3$ independent experiments, in each of which >100 cells were measured. Error bars indicate SD. *, $P < 0.05$ by Student's t test. Bars: (B, H, and I) 20 µm; (C and D) 10 µm.

localized there in Patj-depleted cells (Fig. 6 H), suggesting that cingulin might not mainly serve as a targeting molecule of p114RhoGEF.

We next investigated the role of Patj in the organization of the circumferential actomyosin belt. By Patj depletion, the circumferential actomyosin belt was severely disrupted as with p114RhoGEF depletion: bundles of F-actin and myosin IIA along the apical cell–cell boundaries were mostly lost in Patj-depleted cells (Fig. 6 I). It was also found that Lulu2-induced apical constriction was attenuated in Patj-depleted MDCK cells, suggesting that Patj is required for myosin II regulation by Lulu2 (Fig. 6 J and Fig. S3, H and M). These results suggest that Patj might recruit p114RhoGEF to apical cell–cell boundaries and thereby regulate the integrity of the circumferential actomyosin belt, although we cannot exclude the possibility that Par3 also plays some role in targeting p114RhoGEF.

The FA domain of Lulu2 is phosphorylated by aPKC

Although we showed that the FERM domain of Lulu2 is sufficient for interaction with p114RhoGEF, the role of the FA domain in the regulation of p114RhoGEF remained obscure and was investigated. We noticed that the FA domain of Lulu2 has several potential PKA and PKC phosphorylation sites (Fig. 7 A) and hypothesized that Lulu2 might be regulated by phosphorylation of these sites. To examine whether PKA and PKC phosphorylate Lulu2, we performed phosphate affinity gel electrophoresis of GST-fused proteins subjected to in vitro kinase assays using the acrylamide-pendant Phos-tag ligand followed by immunoblotting with an antibody for GST. In this way, we can detect a phosphorylated protein by retarding its mobility in electrophoresis (Kinoshita et al., 2006). Using this method, it was found that aPKC (PKC-ζ), conventional PKC (PKC-α), and PKA phosphorylate the FA domain. These kinases could efficiently phosphorylate the GST-fused FA domain and GST-fused FERM-FA domain but not the GST-fused FERM domain in vitro (Fig. 7 B and Fig. S4, B and D–G).

As we found that aPKC and its activator Par6, both well-known cell polarity regulators (Suzuki and Ohno, 2006; Goldstein and Macara, 2007; Assémat et al., 2008; Martin-Belmonte and Mostov, 2008; Pieczynski and Margolis, 2011) bind to Myc-Lulu2 (Fig. 7 C), and aPKC can often be detected as a complex with its substrates, we focused on aPKC. There are two aPKCs, PKC-λ and PKC-ζ, which are thought to play redundant roles. Using mutant forms of the FA domain, in which potential PKC phosphorylation sites were replaced by alanines, it was found that Ser385, Ser414, Ser419, and Thr424 were phosphorylated by aPKC in vitro (Fig. 7 D and Fig. S4, H and I). In addition, the phosphorylation of Lulu2 expressed in MDCK cells, which mainly express PKC-λ (not depicted; Suzuki et al., 2004), was markedly reduced by PKC-λ depletion (Fig. 7 E), confirming an aPKC-mediated phosphorylation of Lulu2 in the cells.

aPKC negatively regulates Lulu2 activity

To examine the effect of phosphorylation on Lulu2 activity, we prepared a phosphorylation-mimicking (Lulu2 4E) and a phosphorylation-deficient (Lulu2 4A) form of full-length Lulu2, in which the aforementioned four aPKC phosphorylation sites were replaced by glutamic acids or alanines and tested them for the ability to induce apical constriction (Fig. 8 A). It was found that whereas wild-type Lulu2 and Lulu2 4A induced strong apical constriction in MDCK cells, Lulu2 4E did not (Fig. 8 A), suggesting that the phosphorylation of these sites might negatively regulate Lulu2 activity.

EGFP-tagged wild-type Lulu2 efficiently accumulated along cell–cell boundaries marked by ZO-1 staining like endogenous Lulu2 (Fig. S5). Lulu2 4A also accumulated there. In contrast, Lulu2 4E less efficiently accumulated there: it was detected diffusely in the cytoplasm (Fig. S5). Although these results suggest that Lulu2 localization is regulated by phosphorylation, endogenous Lulu2 localization along apical cell–cell boundaries was not significantly changed in aPKC dominant negative (DN)–expressing cells (unpublished data), suggesting that fine, but as yet unknown, regulation might operate to regulate endogenous Lulu2 localization.

To examine the relationship between Lulu2 and aPKC in the cells, a kinase-deficient form of aPKC, which is thought to function as an aPKC DN (Suzuki et al., 2001), was expressed in the cells. aPKC DN induced apical constriction like Lulu2 in DLD-1 cells (Fig. 8 B). aPKC DN also induced stronger apical constriction in Lulu2-expressing MDCK cells than in parental MDCK cells (Fig. 8 C). These results suggest that aPKC might counteract Lulu2 activity.

In addition, it was found that the phosphorylation of FERM-FA by aPKC markedly reduced its ability to interact with p114RhoGEF (Fig. 8 D). Furthermore, aPKC-phosphorylated Lulu2 scarcely activated p114RhoGEF in vitro (Fig. 8 E). Lulu2 4A bound to p114RhoGEF, whereas Lulu2 4E scarcely bound, further supporting the notion that phosphorylation negatively regulates the interaction (Fig. 8 F). Because Lulu2 normally accumulated along apical cell–cell boundaries in p114RhoGEF-depleted DLD-1 cells (unpublished data), p114RhoGEF is not likely to anchor Lulu2 there. These results together suggest that phosphorylation of the FA domain by aPKC might negatively regulate Lulu2 activity on the circumferential actomyosin belt.

aPKC regulates the circumferential actomyosin belt as well as tight junction

We next conducted aPKC (PKC-λ) RNAi experiments in DLD-1 and MDCK cells. aPKC was, as reported previously for other cell types, localized along apical cell–cell boundaries as well as at the apical membrane in both cells (unpublished data). By aPKC depletion, both the circumferential actomyosin belt and tight junction marked by ZO-1 were severely disrupted in DLD-1 cells and MDCK cells overexpressing Myc-Lulu2 but not in parental MDCK cells (Fig. 8, G and H; and Fig. S3, K and L, RNAi). Consistent with these results, when aPKC DN-expressing cells formed a cell cluster, apical junctions in the cluster were severely disrupted in DLD-1 cells and MDCK cells expressing Myc-Lulu2 but not in parental MDCK cells (unpublished data). These results suggest that cells with high Lulu2 activity, such as DLD-1 cells and MDCK cells expressing Myc-Lulu2, require aPKC activity to properly maintain the apical junctions and the circumferential actomyosin belt.

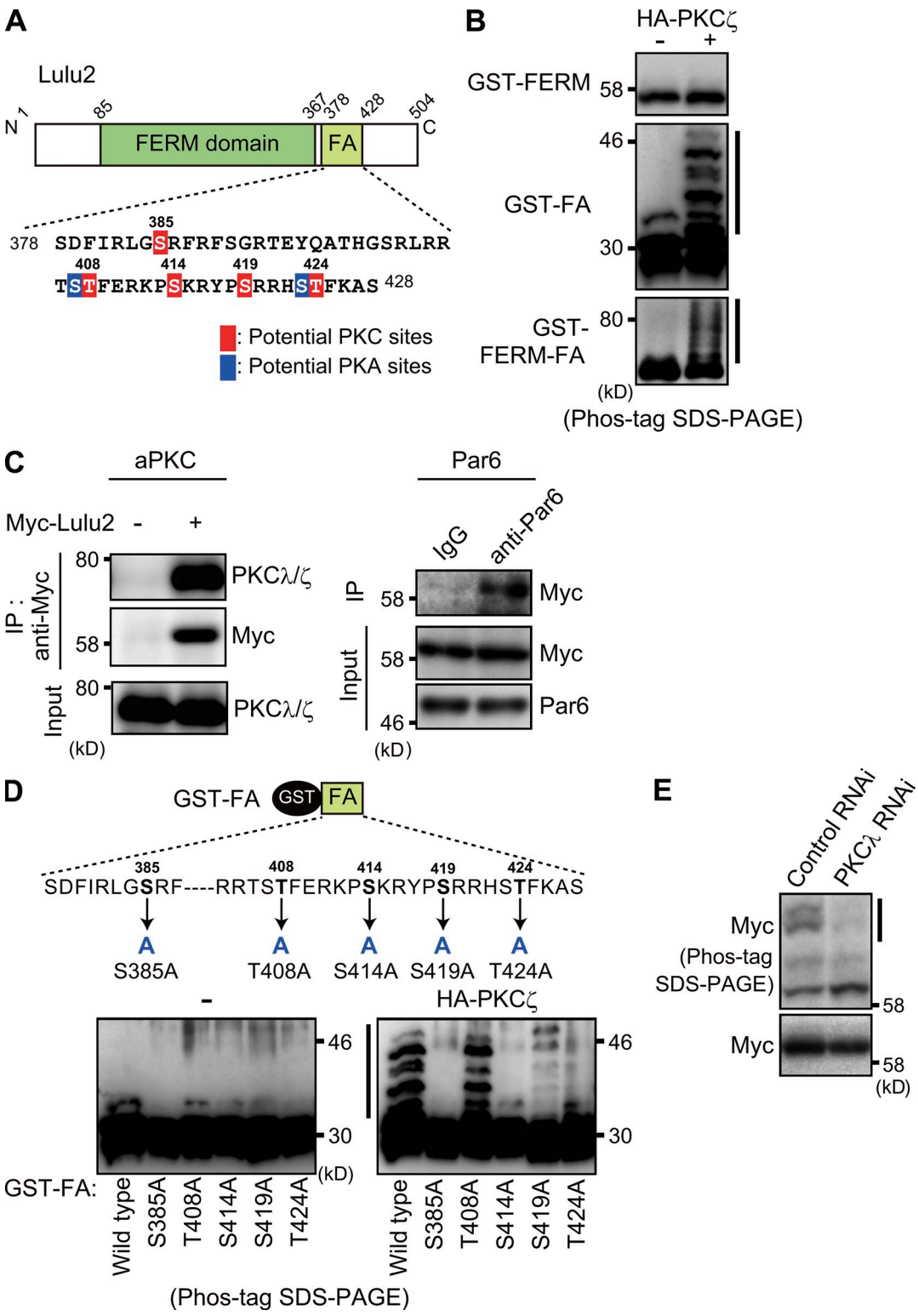

Figure 7. **Lulu2 is phosphorylated by aPKC.** (A) Amino acid sequence of the FA domain (378–428 aa; mouse Lulu2) is shown. Potential PKA or PKC phosphorylation sites (NetPhosK program) are in blue or red, respectively. N, N terminus; C, C terminus. (B) GST-FERM-FA, GST-FERM domain and GST-FA domain were subjected to in vitro kinase assays with PKC-ζ. Phosphorylation was detected by mobility shift patterns (bars) in Mn^{2+}–Phos-tag SDS-PAGE followed by immunoblotting with anti-GST antibody. PKC-ζ used is shown in Fig. S4 E. See Materials and methods for details. (C, left) Lysates of MDCK cells expressing Myc-Lulu2 were immunoprecipitated (IP) with anti-Myc antibody. (left, top, PKC-λ/ζ) Coprecipitated endogenous PKC-λ/ζ was detected. (right) Lysates of MDCK cells expressing Myc-Lulu2 were immunoprecipitated with rabbit control IgG or anti-Par6 antibody. (top right, Myc) Coprecipitated Myc-Lulu2 was detected. (D) GST-fused mutant forms of the FA domain, in which Ser385, Thr408, Ser414, Ser419, or Thr424 was replaced by alanine, were prepared and examined for phosphorylation by aPKC-ζ in vitro (right, HA–PKC-ζ), or left untreated (left, −). Phosphorylated GST-FA was detected by mobility shift patterns (bar) in Mn^{2+}–Phos-tag SDS-PAGE followed by immunoblotting with anti-GST antibody. (E) MDCK cells expressing Myc-Lulu2 were treated with control siRNA or PKC-λ siRNA-1. Phosphorylated Lulu2 was detected by mobility shift patterns (bar) in Mn^{2+}–Phos-tag SDS-PAGE followed by immunoblotting with anti-Myc antibody.

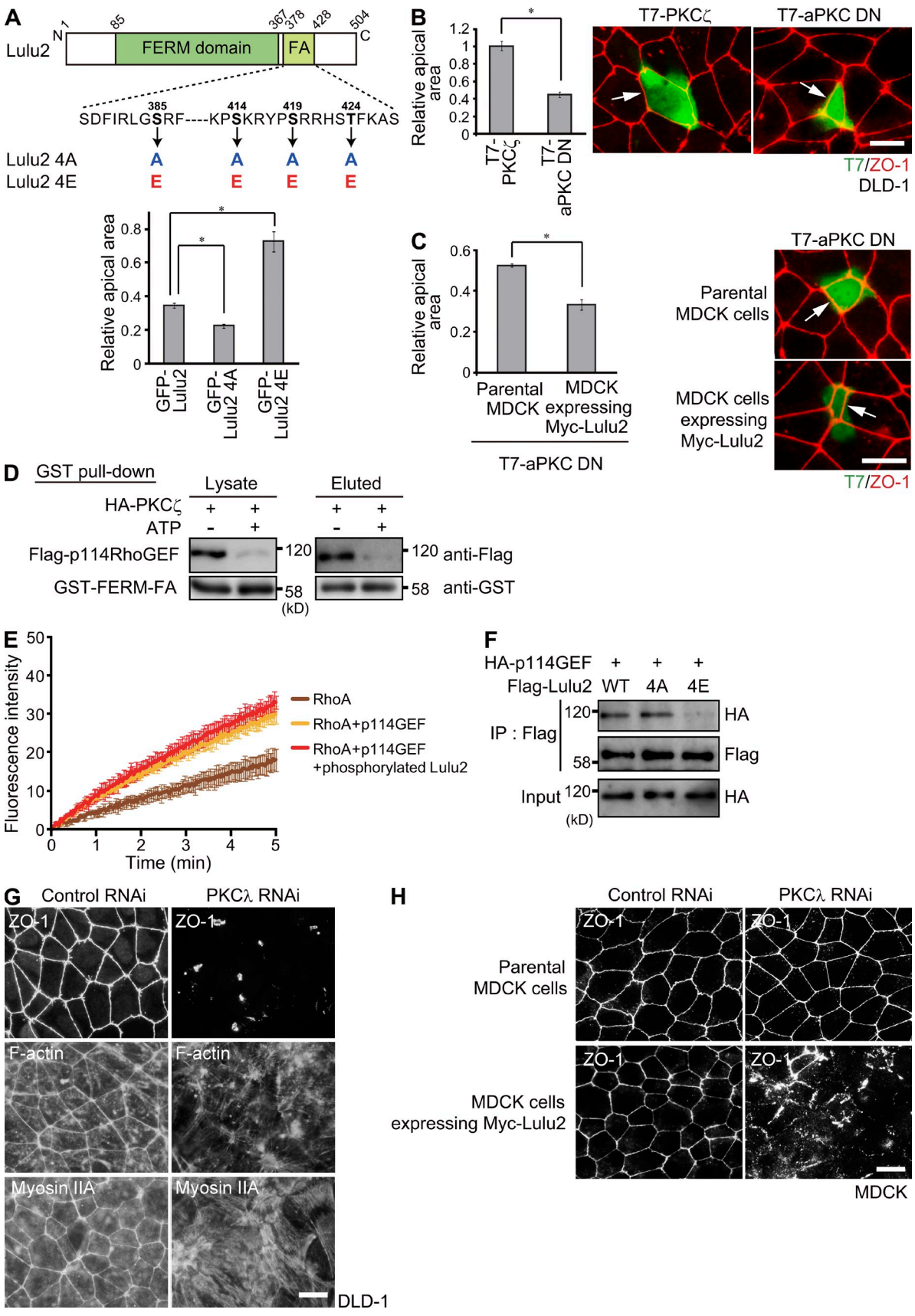

Figure 8. **Lulu2 is negatively regulated by aPKC.** (A) Quantification of apical areas defined by ZO-1 staining signals in EGFP-Lulu2–, EGFP-Lulu2 4A–, or EGFP-Lulu2 4E–expressing cells. Relative apical areas in Lulu2-expressing cells normalized by those in neighboring cells were quantified as in Fig. 4 B. MDCK cells were used. N, N terminus; C, C terminus. (B and C) DLD-1 cells transfected with T7-tagged wild-type aPKC-ζ or dominant-negative aPKC (aPKC DN)

Discussion

We previously reported that Lulu2 overexpression in epithelial cells caused strong accumulation of actomyosin bundles at the cell cortex and induced apical constriction (Nakajima and Tanoue, 2010). Here, we characterized Lulu2 as a regulator of the circumferential actomyosin belt in epithelial cells by studying Lulu2 in more detail at the molecular level. One of the main findings of our present study is that Lulu2 interacts with and activates p114RhoGEF in its regulation of the circumferential actomyosin belt (Fig. 9). p114RhoGEF was recently shown to be an essential regulator of RhoA at apical junctions: it activates RhoA at apical junctions, thereby regulating the circumferential actomyosin belt and participating in tight junction formation in Ca^{2+} switch experiments (Terry et al., 2011). Our results here also confirm the importance of p114RhoGEF in organization of the circumferential actomyosin belt. Its role in tight junction organization, however, might be cell-type dependent: without Ca^{2+} switch, p114RhoGEF depletion resulted in disruption of tight junctions in human corneal epithelial cells but not in Caco2 and DLD-1 cells (Fig. 4; Terry et al., 2011).

p114RhoGEF was reported to play multiple cellular roles depending on cell types and to interact with several molecules. p114RhoGEF participates in stress fiber formation and reactive oxygen species production via binding to Sept9 or the Gβγ subunit of heterotrimeric G proteins in fibroblasts (Niu et al., 2003; Nagata and Inagaki, 2005) and also in neurite elongation via binding to Disheveled and Daam1in neuroblastoma cells (Tsuji et al., 2010). Recently, it was also reported that p114RhoGEF forms a complex with cingulin, myosin II, and Rock II and regulates RhoA activity at apical cell–cell junctions in epithelial cells (Terry et al., 2011). Of note, cingulin interacts with the PH domain of p114RhoGEF at apical cell–cell boundaries in epithelial cells, and its depletion resulted in delocalization of p114RhoGEF from there (Terry et al., 2011). On the other hand, our results show that p114RhoGEF might be recruited to apical cell–cell boundaries by Patj via PDZ domain–mediated interaction; therefore, Patj and cingulin might cooperatively recruit p114RhoGEF to apical cell–cell boundaries in an as yet unknown fashion. Other known p114RhoGEF-interacting molecules also could interact with and regulate p114RhoGEF at apical cell–cell boundaries in epithelial cells, although these possibilities have not been tested yet. Furthermore, Patj, which has 10 PDZ domains, also has several interacting molecules, including Pals1, angiomotin, JAM1, ZO-3, nectins, and Par6, at apical cell–cell boundaries (Lemmers et al., 2002; Roh et al., 2002; Hurd et al., 2003; Michel et al., 2005; Shin et al., 2005; Wells et al., 2006; Massey-Harroche et al., 2007; Sugihara-Mizuno et al., 2007; Adachi et al., 2009). We can thus speculate that there might exist a large molecular complex containing p114RhoGEF at apical cell–cell boundaries and that the components of the complex might cooperatively regulate p114RhoGEF depending on cellular conditions. Our results here show that Lulu2 up-regulates the activity of p114RhoGEF by binding to it. Considering the aforementioned possible complex regulation of p114RhoGEF in the cells, Lulu2, however, might not only activate p114RhoGEF through the simple interaction shown here but also cooperatively regulate it with other unidentified regulators. Therefore, comprehensive identification and characterization of the possible large molecular machinery containing p114RhoGEF and Patj are needed in our future study to fully understand the molecular mechanisms regulating the circumferential actomyosin belt.

FERM domain–containing molecules are also generally thought to play multiple roles and have several interacting

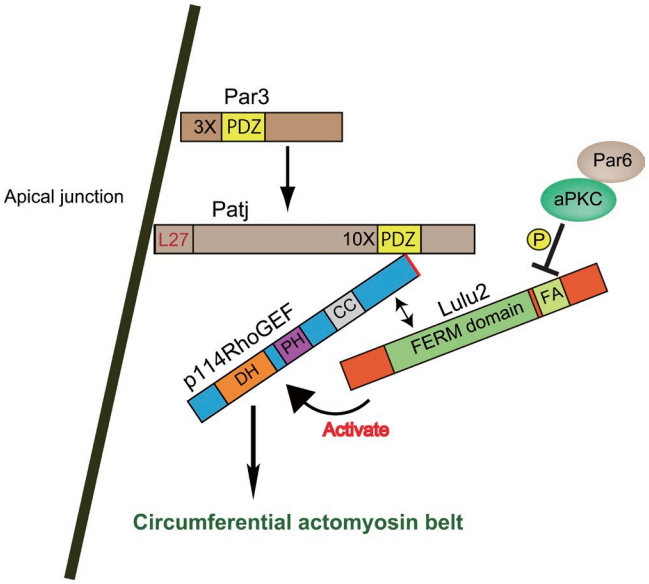

Figure 9. **Schematic representation of Lulu2 involvement in regulation of the circumferential actomyosin belt.** Lulu2 activates p114RhoGEF, thereby regulating the circumferential actomyosin belt. Lulu2 is phosphorylated in the FA domain and negatively regulated by aPKC. p114RhoGEF is recruited to apical cell–cell boundaries by Patj via PDZ domain–mediated interaction. Par3 regulates Patj accumulation at apical cell–cell boundaries. P, phosphorylation; DH, Dbl homology domain; PH, pleckstrin homology domain; CC, coiled-coil region.

were stained for T7 and ZO-1 (B). Parental or Lulu2-expressing MDCK cells were transfected with T7–aPKC DN and stained for T7 and ZO-1 (C). Relative apical areas in aPKC-expressing cells normalized by those in neighboring cells were quantified as in Fig. 4 B. Singly locating aPKC-expressing cells surrounded by nonexpressing cells were measured. Arrows show T7-aPKC–expressing cells. (D) GST-FERM-FA phosphorylated by aPKC-ζ was examined for binding to p114RhoGEF by GST pull-down assays. Phosphorylated (ATP+) or unphosphorylated (ATP−) GST-FERM-FA was incubated with lysates of MDCK cells expressing Flag-p114RhoGEF (Lysate) or with eluted Flag-p114RhoGEF (Eluted). Coprecipitated Flag-p114RhoGEF was detected by anti-Flag antibody. See Materials and methods for details. (E) In vitro guanine nucleotide exchange reaction of p114RhoGEF toward RhoA. aPKC-phosphorylated Lulu2 was incubated with p114RhoGEF (red). See Materials and methods for details. (F) Flag-tagged wild-type Lulu2, Lulu2 4A, and Lulu2 4E were examined for binding to HA-tagged p114RhoGEF in coimmunoprecipitation (IP) assays. Coprecipitated HA-p114RhoGEF was detected (HA). (G) DLD-1 cells treated with control siRNA or PKC-λ siRNA-1 were stained for ZO-1, F-actin, or myosin IIA. (H) Parental MDCK cells or MDCK cells overexpressing Myc-Lulu2 treated with control siRNA or PKC-λ siRNA-1 were stained for ZO-1. $n = 3$ independent experiments, in each of which >50 cells were measured. Error bars indicate SD. *, $P < 0.05$ by Student's t test. Bars, 20 µm.

molecules according to the cellular processes in which they participate (Tepass, 2009; Fehon et al., 2010). Lulu2 might also participate in other cellular processes besides the regulation of the circumferential actomyosin belt. Supporting this notion, Lulu2 is detected not only along apical cell–cell boundaries but also in the cytoplasm as dots, and our screening for interacting molecules of Lulu2 also identified several molecules besides p114RhoGEF, although we did not confirm these interactions in this study. Lulu2 could regulate or be regulated by these molecules in as yet unidentified cellular processes. Although we cannot therefore exclude from our results the possibility that other unidentified binding partners of Lulu2 in addition to p114RhoGEF could also participate in the regulation of the circumferential actomyosin belt, we can conclude that p114RhoGEF is the major downstream target of Lulu2 in the regulation of the circumferential actomyosin belt.

At apical cell–cell boundaries, Lulu2 interacts with p114RhoGEF and p114RhoGEF interacts with Patj. However, Lulu2 is not likely to form such a tight molecular complex with p114RhoGEF that regulates the localization of Lulu2: p114RhoGEF depletion did not alter Lulu2 localization and vice versa. Lulu2 therefore might be recruited to apical cell–cell boundaries by an as yet unidentified molecule/mechanism and associate with, but not be anchored by, p114RhoGEF at apical cell–cell boundaries.

The circumferential actomyosin belt is positioned along the apical cell–cell boundaries, close to both the zonula adherens and tight junction, although the majority of the actomyosin fibers are localized near the zonula adherens (Ivanov et al., 2007; Yamazaki et al., 2008; Smutny et al., 2010; Yonemura et al., 2010). Our results show that Patj and aPKC, both known to accumulate at the level of the tight junction, not the zonula adherens, regulate the circumferential actomyosin belt. It was also reported that ZO-1 and ZO-2, scaffolding molecules at the tight junction, are required for proper organization of the circumferential actomyosin belt and the zonula adherens as well as the tight junction itself (Yamazaki et al., 2008). It could thus be speculated that molecules associated with the tight junction might regulate the proper organization of the circumferential actomyosin belt. On the other hand, E-cadherin, the main component of the zonula adherens, also regulates the circumferential actomyosin belt (Shewan et al., 2005; Smutny et al., 2010). Conversely, the circumferential actomyosin belt also regulates proper organization of the zonula adherens (Shewan et al., 2005; Ivanov et al., 2007; Smutny et al., 2010). Therefore, the formation and maintenance of these three structures, the tight junction, zonula adherens, and the circumferential actomyosin belt, are obviously mutually dependent. Temporal and spatial fine regulations thus should exist to properly regulate their organization. Studying the Lulu2-p114RhoGEF system in more detail might contribute to understanding the regulation of these pivotal architectures in polarized epithelial cells.

The circumferential actomyosin belt serves as a major generator of mechanical force during animal morphogenesis. Accordingly, it should not be a static structure but rather dynamic and flexible. Several signaling pathways might regulate it at an appropriate time and place. From this viewpoint, our findings concerning phosphorylation-mediated Lulu2 regulation might be of importance. We found that aPKC, an apicobasal cell polarity regulator, phosphorylates and negatively regulates Lulu2. In accordance with our results, it was also reported that aPKC antagonizes myosin II activity of the circumferential actomyosin belt (Kishikawa et al., 2008; Mashukova et al., 2011). To establish the epithelial cell structure, regulation of the circumferential actomyosin belt and apicobasal cell polarity might not be independent but interdependent events. The aPKC–Lulu2 pathway might thus be one of the connections between these two cellular processes. In the regulation of myosin II activity of the belt, Lulu2 is obviously not a sole target of aPKC. It was recently reported that aPKC phosphorylates and inhibits Rock1 from accumulating to the apical junctions, thereby negatively regulating myosin II activity of the belt (Ishiuchi and Takeichi, 2011). How these two systems, aPKC–Lulu2-p114RhoGEF and aPKC-Rock1, are spatiotemporally regulated might be an interesting future problem to be addressed. In addition, we found that conventional PKC and PKA also phosphorylate the FA domain of Lulu2, although we did not explore the functional relevance of these phosphorylations in this study. Because both kinases are downstream of several extracellular stimuli, it would be important to identify the stimuli that lead to the phosphorylation of Lulu2 by these kinases in future studies.

In summary, we demonstrated here that the Lulu2-p114RhoGEF system is a regulator of the circumferential actomyosin belt. We further showed that aPKC and Patj, apical cell polarity regulators, regulate the circumferential actomyosin belt through the Lulu2-p114RhoGEF system, at least in part. Elucidating the more detailed mechanisms regulating the Lulu2-p114RhoGEF system is a future important challenge to understand epithelial cell shape regulation.

Materials and methods

Cell culture and immunostaining

MDCK cells (Tet-Off; Takara Bio Inc.) and DLD-1 cells, human colon epithelial cells, were cultured in a 1:1 mixture of DME and Ham's F12 medium (Wako Chemicals USA) supplemented with 10% fetal calf serum. These cells were maintained in 5% CO_2 at 37°C. The stable MDCK Tet-Off Lulu2 transfectants were cultured in the presence of 1 µg/ml doxycycline (Takara Bio Inc.). To induce the expression of Lulu2, the cells were washed twice at 12-h intervals and cultured in doxycycline-free medium for 2–3 d. Cells were transfected using a reagent (Lipofectamine LTX; Invitrogen) according to the manufacturer's protocol. Immunostaining was performed as follows: in brief, cells were fixed with 1 or 3.7% formaldehyde in PBS for 10 min at RT. The fixed cells were then permeabilized with 0.2% Triton X-100 in PBS for 10 min and blocked with 3% BSA in PBS for 30 min at 37°C. Thereafter, the cells were incubated with the appropriate antibodies in 3% BSA in PBS for 1.5 h at 37°C. Next, the cells were washed five times with PBS and incubated with fluorochrome-conjugated secondary antibodies (1:400, Alexa Fluor secondary antibodies; Invitrogen or Jackson ImmunoResearch Laboratories, Inc.) in 3% BSA in PBS for 1 h at 37°C. After five washes with PBS and then rinsing in water (Milli-Q; Millipore), coverslips were mounted with Mowiol (EMD). Alexa Fluor 488 phalloidin (1:200; Invitrogen) was used to visualize F-actin. Images were taken with a microscope (BX51; Olympus) equipped with a charge-coupled device camera system (DP71; Olympus) at RT. A UPlanSApo 20×/0.75 NA lens and a UPlanSApo 40×/0.95 NA lens (Olympus) were used. Images were analyzed with DP Manager software (Olympus) and Photoshop (Adobe). Confocal images were taken with a laser-scanning confocal microscope (LSM510; Carl Zeiss) mounted on an inverted microscope (Axiovert 200M; Carl Zeiss) using a Plan Apochromat

63×/1.40 NA objective and LSM510 software (Carl Zeiss) at RT. Images were analyzed with the same software and with Photoshop software or ImageJ (National Institutes of Health). The apical area of MDCK cells was measured using ImageJ software. Fluorescent intensities were measured by counting gradient values using ImageJ software.

Antibodies

The following antibodies were used: mouse monoclonal antibodies against β-catenin (BD), ZO-1 (Invitrogen), CASK (Millipore), Dlg1 (Santa Cruz Biotechnology, Inc.), Flag (M2; Sigma-Aldrich), GST (Nacalai), PKC-λ (BD), Scribble (Santa Cruz Biotechnology, Inc.), α-tubulin (Sigma-Aldrich), maltose-binding protein (MBP; New England Biolabs, Inc.), Myc (9E10; Santa Cruz Biotechnology, Inc.), and MUPP1 (BD); rat monoclonal antibody against GFP (Nacalai); rabbit polyclonal antibodies against Afadin (Sigma-Aldrich), α-catenin (Sigma-Aldrich), cingulin (Invitrogen), p114RhoGEF (Gentex), ZO-1 (Invitrogen), ZO-2 (Invitrogen), MAGI-1 (Sigma-Aldrich), myosin IIA (Sigma-Aldrich), diphosphorylated MRLC (Cell Signaling Technology), Flag (Sigma-Aldrich), HA (MBL International), Myc (Santa Cruz Biotechnology, Inc.), Par3 (Millipore), Pals1 (Millipore), GST (MBL International), Par6 (Sigma-Aldrich), aPKC-λ/ζ (Santa Cruz Biotechnology, Inc.), Patj (Abcam), T7 (MBL International), and GFP (MBL International); goat polyclonal antibody against Lulu2/Ehm2 (Abcam); control goat IgG (Santa Cruz Biotechnology, Inc.); and control rabbit IgG (Santa Cruz Biotechnology, Inc.). Rabbit anti-Patj antibody used for immunostaining was a gift from A. Le Bivic (Centre National de la Recherche Scientifique, Marseille, France). Rabbit anti-Lulu2 antibody used in the immunoprecipitation assay in Fig. 2 D was raised against mouse Lulu2/Ehm2 peptide (451–466 aa). Primary antibodies were visualized with goat or chicken fluorochrome-conjugated secondary antibodies. The fluorochromes used were Alexa Fluor 488, 549, 555, and 568 (Invitrogen or Jackson ImmunoResearch Laboratories, Inc.).

Plasmid construction and protein expression

Mouse cDNA of Lulu2-S, the short form of Lulu2 (Nakajima and Tanoue, 2010), was provided by J. Yokota (National Cancer Center Research Institute, Tokyo, Japan). Lulu2 has two alternatively spliced transcripts that share FERM and FA domains in their N-terminal portions (Nakajima and Tanoue, 2010). The full-length form of Lulu2-S was cloned into pEGFP-C1 (Takara Bio Inc.), pFlag-cytomegalovirus (CMV)-6C (Sigma-Aldrich), pCMV-3Tag-2 (Agilent Technologies), or pTRE2hyg (Takara Bio Inc.), in which three Myc tags were attached to the N terminus. The FERM (85–367 aa), FERM-FA (85–428 aa), and FA (378–428 aa) domains of Lulu2 were obtained by PCR and cloned into pEGFP-C1. Full-length human cDNA of p114RhoGEF was obtained by PCR from a cDNA template (KIAA0521; Kazusa DNA Research Institute) and then cloned into pEGFP-C2 (Takara Bio Inc.), pFlag-CMV-6C, or pTRE2hyg, in which a Flag tag was attached to the N terminus. Truncated mutant forms of p114RhoGEF (N-terminal domain: 1–441 aa; C-terminal domain: 452–1,015 aa; C1: 452–643 aa; C2: 644–1,015 aa; C2ΔPBM: 644–1,009 aa; C3: 633–800 aa; C4: 799–1,015 aa; C4ΔPBM: 799–1,009 aa; and FLΔPBM: 1–1,009) were cloned into pEGFP-C2 or pGEX-4T-1 (GE Healthcare). pTB701-HA–PKC-α was a gift from N. Saito (Kobe University, Kobe, Japan). pGEX-2T-RhoA was a gift from K. Kaibuchi (Nagoya University, Chikusa-ku, Nagoya, Japan). pCAGGS-Myc-Par3, pCAGGS-HA–aPKC-ζ and pCAGGS-Patj-Myc were gifts from M. Adachi (Kyoto University, Kyoto, Japan). SRHisB-T7–aPKC-λ and SRHisB-T7–aPKC-λ K273E (aPKC DN) were gifts from S. Ohno (Yokohama City University, Hodogaya-ku, Yokohama, Japan). pGEX-4T1 or pGEX-4T3 vector (GE Healthcare) was used to produce GST-fused various mutant of Lulu2 and p114RhoGEF in *Escherichia coli*. For MBP-fused protein production in *E. coli*, pMAL-c2 vector (New England Biolabs, Inc.) was used.

Mutagenesis

The mutants used were constructed by PCR-based mutagenesis. PCR was performed using DNA polymerase (PfuTurbo; Agilent Technologies). A DpnI restriction enzyme (Agilent Technologies)–treated PCR product was transformed into *E. coli*. Positive clones were selected, and mutagenesis was verified by sequencing.

RNAi

Stealth RNAi negative control (Invitrogen) was used for control RNAi. Transfection of Stealth siRNA was performed using a reagent (RNAiMAX; Invitrogen). In each RNAi experiment, essentially the same results were obtained using two independent RNAi sequences. The following Stealth siRNA were used for RNAi experiments: Lulu2 siRNAi-1 (human), 5′-CACCUUUGAGAGGAAGCCUAGUAAA-3′; Lulu2 siRNAi-2 (human), 5′-CGGAGACAUUCAACGUUCAAAGCAA-3′; p114RhoGEF siRNAi-1 (human), 5′-UGGCCACAAUGAAGCUGUUAGUCAU-3′; p114RhoGEF siRNAi-2 (human), 5′-GAUGGACCUGAAGUCUUCCAGCAAA-3′; Par3 siRNAi-1 (human), 5′-CAAGCCAUGCGUACACCCAUCAUUU-3′; Par3 siRNAi-2 (human), 5′-CCUGAGCAGAUAGACUCUCACUCAA-3′; Patj siRNAi-1 (human), 5′-GCAGAUGAUGCUGAGUUACAGAAAU-3′; Patj siRNAi-2 (human), 5′-GCAUGAAUUUCUGACUCCUAGAUUG-3′; Patj siRNAi-1 (canine), 5′-UGGAGCAGUGGAAACGGAAACUAAU-3′; Patj siRNAi-2 (canine), 5′-GCAGAUGAUGCUGAGUUACAGAAAU-3′; p114RhoGEF siRNAi-1 (canine), 5′-UGGCCACAAUGAGGCGGUCAAUCAU-3′; p114RhoGEF siRNAi-2 (canine), 5′-GGCCAACGAGGAGAAAGCCAUGUUU-3′; PKC-λ siRNAi-1 (canine and human), 5′-CAGAGGAUUAUCUCUUCCAAGUUAU-3′; and PKC-λ siRNAi-2 (canine and human), 5′-AGGAGAAGAUUAUGGUUUCAGUGUU-3′.

Western blotting

Cells were homogenized or lysed in 20 mM Tris-HCl, pH 7.4, containing 1.5 mM $MgCl_2$, 1.5 mM EGTA, 150 mM NaCl, 0.5% NP-40, 10% glycerol, 1 mM phenylmethylsulfonyl fluoride, and 20 µg/ml aprotinin. For Mn^{2+}–Phos-tag SDS-PAGE, EGTA was not included. Proteins were fractionated by SDS-PAGE using a 7, 10, or 15% gel. Prestained molecular markers (Nacalai or New England Biolabs, Inc.) were used. The fractionated proteins were electroblotted onto polyvinyldifluoride membranes (Immobilon-P; Millipore) using a semidry transfer apparatus (Bio-Rad Laboratories). The membrane was blocked with 2% blocking agent (ECL Advance; GE Healthcare) for 30 min at RT. Proteins were then probed for 16 h at 4°C with an appropriate antibody in 20 mM Tris-HCl, pH 7.4, containing 150 mM NaCl and 3% BSA or in 20 mM Tris-HCl, pH 7.4, containing 150 mM NaCl, 0.05% Tween 20, and 0.2% ECL Advance blocking agent. The membrane was then washed three times at room temperature (15 min each time) in 20 mM Tris-HCl, pH 7.4, containing 150 mM NaCl and 0.05% Tween 20 (TBS-Tween) and was subsequently incubated for 2 h at RT with a secondary antibody in TBS-Tween containing 3% BSA or 2% ECL Advance blocking agent. After three washes with TBS-Tween, the proteins were detected using ECL Advance reagent according to the manufacturer's protocol. Chemiluminescence was detected using an imager (ImageQuant 400; GE Healthcare).

Immunoprecipitation and GST pull-down assay

For immunoprecipitation, the cells were lysed in lysis buffer (20 mM Tris-HCl, pH 7.4, containing 150 mM NaCl, 0.5% NP-40, 1.5 mM $MgCl_2$, 1.5 mM EGTA, 10% glycerol, 1 mM phenylmethylsulfonyl fluoride, and 20 µg/ml aprotinin). Lysates were incubated with an appropriate antibody and protein A–Sepharose (GE Healthcare) or anti-Flag M2 affinity gel (Sigma-Aldrich) for 2 h at 4°C. The beads were subsequently washed three times in lysis buffer.

For GST pull-down assays, cells were lysed in lysis buffer (20 mM Tris-HCl, pH 7.4, containing 150 mM NaCl, 0.5% NP-40, 1.5 mM $MgCl_2$, 1.5 mM EGTA, 10% glycerol,1 mM phenylmethylsulfonyl fluoride and 20 µg/ml aprotinin). GST fusion proteins and glutathione–Sepharose 4B beads (GE Healthcare) were added to the lysate. After a 4-h incubation at 4°C, the beads were washed four times in lysis buffer. The obtained samples were analyzed by Western blotting or LC-MS/MS. For LC-MS/MS, bands identified by staining using an MS-grade silver staining kit (Wako Chemicals USA) or fluorescent gel stain (Oriole; Bio-Rad Laboratories) after SDS-PAGE were analyzed in the Center for Mass Spectrometry at Kobe University Graduate School of Medicine.

Proximity ligation assay

The proximity ligation assay was performed using an in situ proximity ligation assay kit (Duolink II; Olink Bioscience) according to the manufacturer's instructions. The ligation signals indicate the proximity (<40 nm) of secondary antibodies detecting anti-Lulu2 antibodies bound to Lulu2 to those detecting anti-p114RhoGEF antibodies bound to p114RhoGEF.

In vitro binding assay

In Fig. 3 C, GST-tagged C4ΔPBM, GST, MBP-tagged FERM-FA, and MBP were prepared in bacteria. GST-tagged C4ΔPBM or GST (0.2 µg each) was mixed and incubated for 2 h at RT with MBP-tagged FERM or MBP (1 µg each) and then precipitated with amylase/agarose beads (New England Biolabs, Inc.). The beads were subsequently washed three times in TBS (20 mM Tris-HCl, pH 7.4, and 150 mM NaCl). Coprecipitated GST-C4ΔPBM was detected by Western blotting using the anti-GST antibody.

In Fig. 8 D, Flag-p114RhoGEF was immunoprecipitated from lysates of MDCK cells expressing Flag-p114RhoGEF and then eluted with 0.1 mg/ml Flag peptides (Sigma-Aldrich). The eluted Flag-p114RhoGEF protein was incubated with phosphorylated or unphosphorylated GST-FERM-FA

and then precipitated with glutathione-SH beads (GE Healthcare). The beads were subsequently washed three times in the lysis buffer. Coprecipitated Flag-p114RhoGEF was detected by Western blotting using the anti-Flag antibody.

In vitro kinase assay

MDCK cells transfected with pSR-α-HA–PKC-ζ or pTB701-HA–PKC-α were lysed in lysis buffer (20 mM Tris-HCl, pH 7.4, containing 150 mM NaCl, 0.5% NP-40, 1.5 mM $MgCl_2$, 1.5 mM EGTA, 10% glycerol, 1 mM sodium vanadate, 1 mM phenylmethylsulfonyl fluoride, and 20 µg/ml aprotinin). HA-PKC protein was immunoprecipitated from cell lysates (~10^6 cells in each sample) by incubation with 2 µg HA antibody (MBL International) and 15 µl protein A–Sepharose beads for 2 h at 4°C. The precipitate was washed three times with the lysis buffer and then washed with Tris buffer (20 mM Tris-HCl, pH 7.4). The HA-tagged kinases were then eluted with 1 mg/ml HA peptides (Roche). The eluted kinase was mixed with 0.4 µg GST-fused Lulu2 proteins in a kinase reaction buffer (20 mM Tris-HCl, pH 7.5, 12.5 mM $MgCl_2$, 1 mM DTT, 2 mM 2-glycerophosphate, 2 mM sodium vanadate, 10 mM NaF, and 100 µM ATP (Sigma-Aldrich); 10× PKC Lipid Activator (Millipore) and 2 mM $CaCl_2$ were also included for conventional PKC-α) and incubated for 1 h at 30°C for PKC-α or 16 h at 30°C for PKC-ζ. Phosphorylation was detected by Western blotting using the Phos-tag system (Wako Chemicals USA), a detection system of phosphorylated proteins using the dinuclear manganese complex of acrylamide-pendant Phos-tag as a phosphate-binding tag. Phos-tag was used at 25 µM. In Fig. 8 D, 1.5 µg GST-FERM-FA with glutathione-SH beads was incubated with HA–PKC-ζ in the presence (Fig. 8 D, ATP+) or absence (Fig. 8 D, ATP−) of ATP in the kinase reaction buffer and used for the binding assays.

In vitro GEF assay

Flag-tagged p114RhoGEF and Myc-tagged Lulu2 were immunoprecipitated from MDCK cells expressing each protein using anti-Flag M2 affinity gel or Myc (9E10; Santa Cruz Biotechnology, Inc.) antibody. After three washes with lysis buffer, the proteins were eluted with Flag or Myc peptides (Sigma-Aldrich). Amounts of the obtained proteins were routinely determined by Coomassie brilliant blue (CBB) or Oriole staining using BSA as a standard after SDS-PAGE. The obtained proteins were then used for the GEF assay. In Fig. 8 E, immunoprecipitated Myc-tagged Lulu2 with protein A–Sepharose beads was incubated with eluted HA–PKC-ζ in the presence of ATP in the kinase reaction buffer for 3 h at 30°C. After washing three times with TBS, Myc-tagged Lulu2 was eluted with Myc peptides and then used for the GEF assay.

Initially, 2 µM GST-RhoA-GDP was added to the GEF assay buffer (20 mM Tris-HCl, pH 7.5, containing 50 mM NaCl, 10 mM $MgCl_2$, 1 mM DTT, 50 µg/ml BSA, 10% glycerol, and 400 nM *N*-methylanthraniloyl–GTP [Invitrogen]) and equilibrated for 5 min at 25°C. The reaction was initiated by the addition of 0.1 µM p114RhoGEF in the presence or absence of 0.1 µM Lulu2, and fluorescence was monitored at 25°C using a spectrofluorometer (λ_{ex} = 360 nm; λ_{em} = 440 nm; slits = 3/10 nm; FP-6500; JASCO). The guanine nucleotide exchange reaction was monitored as an increase in fluorescence, which is indicative of the binding of *N*-methylanthraniloyl–GTP to GST-RhoA.

Statistical analysis

P-values were calculated by Student's *t* test using Excel (Microsoft).

Online supplemental material

Fig. S1 shows that DLD-1 cells exhibit the characteristic morphology of polarized epithelial cells with a well-developed circumferential actomyosin belt. Fig. S2 shows the characterization of the anti-Lulu2 antibodies and the efficiency of Lulu2 RNAi. Fig. S3 shows the characterization of the anti-p114RhoGEF antibody and the efficiencies of the p114RhoGEF, Patj, Par3, and aPKC RNAi. Fig. S4 shows the CBB images of the bacterially expressed proteins and that Patj and Par3 bound to the C2 region among several PDZ molecules, p114RhoGEF C4ΔPBM bound to Lulu2 FERM in vitro, and PKA and PKC-α, but not CKI-ε, also phosphorylated Lulu2. Fig. S5 shows that exogenously expressed wild-type Lulu2 and Lulu2 4A accumulated along apical cell–cell boundaries, whereas Lulu2 4E did not. Online supplemental material is available at http://www.jcb.org/cgi/content/full/jcb.201104118/DC1.

We thank D. Hamada for access to equipment, T. Otani for technical comments, M. Hayakawa, M. Masuda, H. Koma, M. Wakao, P.T. Chau, and R. Masuhiro for technical support, J. Yokota, M. Adachi, K. Kaibuchi, N. Saito, and S. Ohno for cDNA, and A. Le Bivic for antibodies.

This work was supported by grants from the Global Center of Excellence Program, a Grant-in-Aid for Scientific Research on Innovative Areas, the Inamori Foundation, and Daiichi Sankyo Foundation of Life Science (to T. Tanoue).

Submitted: 22 April 2011
Accepted: 14 September 2011

References

Adachi, M., Y. Hamazaki, Y. Kobayashi, M. Itoh, S. Tsukita, M. Furuse, and S. Tsukita. 2009. Similar and distinct properties of MUPP1 and Patj, two homologous PDZ domain-containing tight-junction proteins. *Mol. Cell. Biol.* 29:2372–2389. http://dx.doi.org/10.1128/MCB.01505-08

Assémat, E., E. Bazellières, E. Pallesi-Pocachard, A. Le Bivic, and D. Massey-Harroche. 2008. Polarity complex proteins. *Biochim. Biophys. Acta*. 1778:614–630. http://dx.doi.org/10.1016/j.bbamem.2007.08.029

Fehon, R.G., A.I. McClatchey, and A. Bretscher. 2010. Organizing the cell cortex: the role of ERM proteins. *Nat. Rev. Mol. Cell Biol.* 11:276–287. http://dx.doi.org/10.1038/nrm2866

García-Mata, R., and K. Burridge. 2007. Catching a GEF by its tail. *Trends Cell Biol.* 17:36–43. http://dx.doi.org/10.1016/j.tcb.2006.11.004

Goldstein, B., and I.G. Macara. 2007. The PAR proteins: fundamental players in animal cell polarization. *Dev. Cell*. 13:609–622. http://dx.doi.org/10.1016/j.devcel.2007.10.007

Hirano, M., S. Hashimoto, S. Yonemura, H. Sabe, and S. Aizawa. 2008. EPB41L5 functions to post-transcriptionally regulate cadherin and integrin during epithelial–mesenchymal transition. *J. Cell Biol.* 182:1217–1230. http://dx.doi.org/10.1083/jcb.200712086

Hoover, K.B., and P.J. Bryant. 2002. *Drosophila* Yurt is a new protein-4.1-like protein required for epithelial morphogenesis. *Dev. Genes Evol.* 212:230–238. http://dx.doi.org/10.1007/s00427-002-0231-6

Hsu, Y.C., J.J. Willoughby, A.K. Christensen, and A.M. Jensen. 2006. Mosaic Eyes is a novel component of the Crumbs complex and negatively regulates photoreceptor apical size. *Development*. 133:4849–4859. http://dx.doi.org/10.1242/dev.02685

Hurd, T.W., L. Gao, M.H. Roh, I.G. Macara, and B. Margolis. 2003. Direct interaction of two polarity complexes implicated in epithelial tight junction assembly. *Nat. Cell Biol.* 5:137–142. http://dx.doi.org/10.1038/ncb923

Ishiuchi, T., and M. Takeichi. 2011. Willin and Par3 cooperatively regulate epithelial apical constriction through aPKC-mediated ROCK phosphorylation. *Nat. Cell Biol.* 13:860–866. http://dx.doi.org/10.1038/ncb2274

Ivanov, A.I., I.C. McCall, C.A. Parkos, and A. Nusrat. 2004. Role for actin filament turnover and a myosin II motor in cytoskeleton-driven disassembly of the epithelial apical junctional complex. *Mol. Biol. Cell*. 15:2639–2651. http://dx.doi.org/10.1091/mbc.E04-02-0163

Ivanov, A.I., M. Bachar, B.A. Babbin, R.S. Adelstein, A. Nusrat, and C.A. Parkos. 2007. A unique role for nonmuscle myosin heavy chain IIA in regulation of epithelial apical junctions. *PLoS ONE*. 2:e658. http://dx.doi.org/10.1371/journal.pone.0000658

Jensen, A.M., and M. Westerfield. 2004. Zebrafish mosaic eyes is a novel FERM protein required for retinal lamination and retinal pigmented epithelial tight junction formation. *Curr. Biol.* 14:711–717. http://dx.doi.org/10.1016/j.cub.2004.04.006

Kinoshita, E., E. Kinoshita-Kikuta, K. Takiyama, and T. Koike. 2006. Phosphate-binding tag, a new tool to visualize phosphorylated proteins. *Mol. Cell. Proteomics*. 5:749–757.

Kishikawa, M., A. Suzuki, and S. Ohno. 2008. aPKC enables development of zonula adherens by antagonizing centripetal contraction of the circumferential actomyosin cables. *J. Cell Sci.* 121:2481–2492. http://dx.doi.org/10.1242/jcs.024109

Laprise, P., S. Beronja, N.F. Silva-Gagliardi, M. Pellikka, A.M. Jensen, C.J. McGlade, and U. Tepass. 2006. The FERM protein Yurt is a negative regulatory component of the Crumbs complex that controls epithelial polarity and apical membrane size. *Dev. Cell*. 11:363–374. http://dx.doi.org/10.1016/j.devcel.2006.06.001

Laprise, P., K.M. Lau, K.P. Harris, N.F. Silva-Gagliardi, S.M. Paul, S. Beronja, G.J. Beitel, C.J. McGlade, and U. Tepass. 2009. Yurt, Coracle, Neurexin IV and the Na(+),K(+)-ATPase form a novel group of epithelial polarity proteins. *Nature*. 459:1141–1145. http://dx.doi.org/10.1038/nature08067

Lecuit, T., and P.F. Lenne. 2007. Cell surface mechanics and the control of cell shape, tissue patterns and morphogenesis. *Nat. Rev. Mol. Cell Biol.* 8:633–644. http://dx.doi.org/10.1038/nrm2222

le Duc, Q., Q. Shi, I. Blonk, A. Sonnenberg, N. Wang, D. Leckband, and J. de Rooij. 2010. Vinculin potentiates E-cadherin mechanosensing and is recruited to actin-anchored sites within adherens junctions in a

myosin II–dependent manner. *J. Cell Biol.* 189:1107–1115. http://dx.doi.org/10.1083/jcb.201001149

Lee, J.D., N.F. Silva-Gagliardi, U. Tepass, C.J. McGlade, and K.V. Anderson. 2007. The FERM protein Epb4.1l5 is required for organization of the neural plate and for the epithelial-mesenchymal transition at the primitive streak of the mouse embryo. *Development*. 134:2007–2016. http://dx.doi.org/10.1242/dev.000885

Lemmers, C., E. Médina, M.H. Delgrossi, D. Michel, J.P. Arsanto, and A. Le Bivic. 2002. hINADl/PATJ, a homolog of discs lost, interacts with crumbs and localizes to tight junctions in human epithelial cells. *J. Biol. Chem.* 277:25408–25415. http://dx.doi.org/10.1074/jbc.M202196200

Martin-Belmonte, F., and K. Mostov. 2008. Regulation of cell polarity during epithelial morphogenesis. *Curr. Opin. Cell Biol.* 20:227–234. http://dx.doi.org/10.1016/j.ceb.2008.01.001

Mashukova, A., F.A. Wald, and P.J. Salas. 2011. Tumor necrosis factor alpha and inflammation disrupt the polarity complex in intestinal epithelial cells by a posttranslational mechanism. *Mol. Cell. Biol.* 31:756–765. http://dx.doi.org/10.1128/MCB.00811-10

Massey-Harroche, D., M.H. Delgrossi, L. Lane-Guermonprez, J.P. Arsanto, J.P. Borg, M. Billaud, and A. Le Bivic. 2007. Evidence for a molecular link between the tuberous sclerosis complex and the Crumbs complex. *Hum. Mol. Genet.* 16:529–536. http://dx.doi.org/10.1093/hmg/ddl485

Michel, D., J.P. Arsanto, D. Massey-Harroche, C. Béclin, J. Wijnholds, and A. Le Bivic. 2005. PATJ connects and stabilizes apical and lateral components of tight junctions in human intestinal cells. *J. Cell Sci.* 118:4049–4057. http://dx.doi.org/10.1242/jcs.02528

Miyake, Y., N. Inoue, K. Nishimura, N. Kinoshita, H. Hosoya, and S. Yonemura. 2006. Actomyosin tension is required for correct recruitment of adherens junction components and zonula occludens formation. *Exp. Cell Res.* 312:1637–1650. http://dx.doi.org/10.1016/j.yexcr.2006.01.031

Nagata, K., and M. Inagaki. 2005. Cytoskeletal modification of Rho guanine nucleotide exchange factor activity: identification of a Rho guanine nucleotide exchange factor as a binding partner for Sept9b, a mammalian septin. *Oncogene*. 24:65–76. http://dx.doi.org/10.1038/sj.onc.1208101

Nakajima, H., and T. Tanoue. 2010. Epithelial cell shape is regulated by Lulu proteins via myosin-II. *J. Cell Sci.* 123:555–566. http://dx.doi.org/10.1242/jcs.057752

Nishimura, T., and M. Takeichi. 2008. Shroom3-mediated recruitment of Rho kinases to the apical cell junctions regulates epithelial and neuroepithelial planar remodeling. *Development*. 135:1493–1502. http://dx.doi.org/10.1242/dev.019646

Niu, J., J. Profirovic, H. Pan, R. Vaiskunaite, and T.G. Voyno-Yasenetskaya. 2003. G Protein betagamma subunits stimulate p114RhoGEF, a guanine nucleotide exchange factor for RhoA and Rac1: regulation of cell shape and reactive oxygen species production. *Circ. Res.* 93:848–856. http://dx.doi.org/10.1161/01.RES.0000097607.14733.0C

Owaribe, K., R. Kodama, and G. Eguchi. 1981. Demonstration of contractility of circumferential actin bundles and its morphogenetic significance in pigmented epithelium in vitro and in vivo. *J. Cell Biol.* 90:507–514. http://dx.doi.org/10.1083/jcb.90.2.507

Pieczynski, J., and B. Margolis. 2011. Protein complexes that control renal epithelial polarity. *Am. J. Physiol. Renal Physiol.* 300:F589–F601. http://dx.doi.org/10.1152/ajprenal.00615.2010

Roh, M.H., O. Makarova, C.J. Liu, K. Shin, S. Lee, S. Laurinec, M. Goyal, R. Wiggins, and B. Margolis. 2002. The Maguk protein, Pals1, functions as an adapter, linking mammalian homologues of Crumbs and Discs Lost. *J. Cell Biol.* 157:161–172. http://dx.doi.org/10.1083/jcb.200109010

Schmidt, A., and A. Hall. 2002. Guanine nucleotide exchange factors for Rho GTPases: turning on the switch. *Genes Dev.* 16:1587–1609. http://dx.doi.org/10.1101/gad.1003302

Shewan, A.M., M. Maddugoda, A. Kraemer, S.J. Stehbens, S. Verma, E.M. Kovacs, and A.S. Yap. 2005. Myosin 2 is a key Rho kinase target necessary for the local concentration of E-cadherin at cell-cell contacts. *Mol. Biol. Cell*. 16:4531–4542. http://dx.doi.org/10.1091/mbc.E05-04-0330

Shimizu, K., Y. Nagamachi, M. Tani, K. Kimura, T. Shiroishi, S. Wakana, and J. Yokota. 2000. Molecular cloning of a novel NF2/ERM/4.1 superfamily gene, ehm2, that is expressed in high-metastatic K1735 murine melanoma cells. *Genomics*. 65:113–120. http://dx.doi.org/10.1006/geno.2000.6154

Shin, K., S. Straight, and B. Margolis. 2005. PATJ regulates tight junction formation and polarity in mammalian epithelial cells. *J. Cell Biol.* 168:705–711. http://dx.doi.org/10.1083/jcb.200408064

Smutny, M., and A.S. Yap. 2010. Neighborly relations: cadherins and mechanotransduction. *J. Cell Biol.* 189:1075–1077. http://dx.doi.org/10.1083/jcb.201005151

Smutny, M., H.L. Cox, J.M. Leerberg, E.M. Kovacs, M.A. Conti, C. Ferguson, N.A. Hamilton, R.G. Parton, R.S. Adelstein, and A.S. Yap. 2010. Myosin II isoforms identify distinct functional modules that support integrity of the epithelial zonula adherens. *Nat. Cell Biol.* 12:696–702. http://dx.doi.org/10.1038/ncb2072

Sugihara-Mizuno, Y., M. Adachi, Y. Kobayashi, Y. Hamazaki, M. Nishimura, T. Imai, M. Furuse, and S. Tsukita. 2007. Molecular characterization of angiomotin/JEAP family proteins: interaction with MUPP1/Patj and their endogenous properties. *Genes Cells*. 12:473–486. http://dx.doi.org/10.1111/j.1365-2443.2007.01066.x

Suzuki, A., and S. Ohno. 2006. The PAR-aPKC system: lessons in polarity. *J. Cell Sci.* 119:979–987. http://dx.doi.org/10.1242/jcs.02898

Suzuki, A., T. Yamanaka, T. Hirose, N. Manabe, K. Mizuno, M. Shimizu, K. Akimoto, Y. Izumi, T. Ohnishi, and S. Ohno. 2001. Atypical protein kinase C is involved in the evolutionarily conserved par protein complex and plays a critical role in establishing epithelia-specific junctional structures. *J. Cell Biol.* 152:1183–1196. http://dx.doi.org/10.1083/jcb.152.6.1183

Suzuki, A., M. Hirata, K. Kamimura, R. Maniwa, T. Yamanaka, K. Mizuno, M. Kishikawa, H. Hirose, Y. Amano, N. Izumi, et al. 2004. aPKC acts upstream of PAR-1b in both the establishment and maintenance of mammalian epithelial polarity. *Curr. Biol.* 14:1425–1435. http://dx.doi.org/10.1016/j.cub.2004.08.021

Tepass, U. 2009. FERM proteins in animal morphogenesis. *Curr. Opin. Genet. Dev.* 19:357–367. http://dx.doi.org/10.1016/j.gde.2009.05.006

Terry, S.J., C. Zihni, A. Elbediwy, E. Vitiello, I.V. Leefa Chong San, M.S. Balda, and K. Matter. 2011. Spatially restricted activation of RhoA signalling at epithelial junctions by p114RhoGEF drives junction formation and morphogenesis. *Nat. Cell Biol.* 13:159–166. http://dx.doi.org/10.1038/ncb2156

Tsuji, T., Y. Ohta, Y. Kanno, K. Hirose, K. Ohashi, and K. Mizuno. 2010. Involvement of p114-RhoGEF and Lfc in Wnt-3a- and dishevelled-induced RhoA activation and neurite retraction in N1E-115 mouse neuroblastoma cells. *Mol. Biol. Cell*. 21:3590–3600. http://dx.doi.org/10.1091/mbc.E10-02-0095

Wells, C.D., J.P. Fawcett, A. Traweger, Y. Yamanaka, M. Goudreault, K. Elder, S. Kulkarni, G. Gish, C. Virag, C. Lim, et al. 2006. A Rich1/Amot complex regulates the Cdc42 GTPase and apical-polarity proteins in epithelial cells. *Cell*. 125:535–548. http://dx.doi.org/10.1016/j.cell.2006.02.045

Yamazaki, Y., K. Umeda, M. Wada, S. Nada, M. Okada, S. Tsukita, and S. Tsukita. 2008. ZO-1- and ZO-2-dependent integration of myosin-2 to epithelial zonula adherens. *Mol. Biol. Cell*. 19:3801–3811. http://dx.doi.org/10.1091/mbc.E08-04-0352

Yano, T., Y. Yamazaki, M. Adachi, K. Okawa, P. Fort, M. Uji, S. Tsukita, and S. Tsukita. 2011. Tara up-regulates E-cadherin transcription by binding to the Trio RhoGEF and inhibiting Rac signaling. *J. Cell Biol.* 193:319–332. http://dx.doi.org/10.1083/jcb.201009100

Yonemura, S., Y. Wada, T. Watanabe, A. Nagafuchi, and M. Shibata. 2010. alpha-Catenin as a tension transducer that induces adherens junction development. *Nat. Cell Biol.* 12:533–542. http://dx.doi.org/10.1038/ncb2055

Zallen, J.A., and J.T. Blankenship. 2008. Multicellular dynamics during epithelial elongation. *Semin. Cell Dev. Biol.* 19:263–270. http://dx.doi.org/10.1016/j.semcdb.2008.01.005